CHALMERS

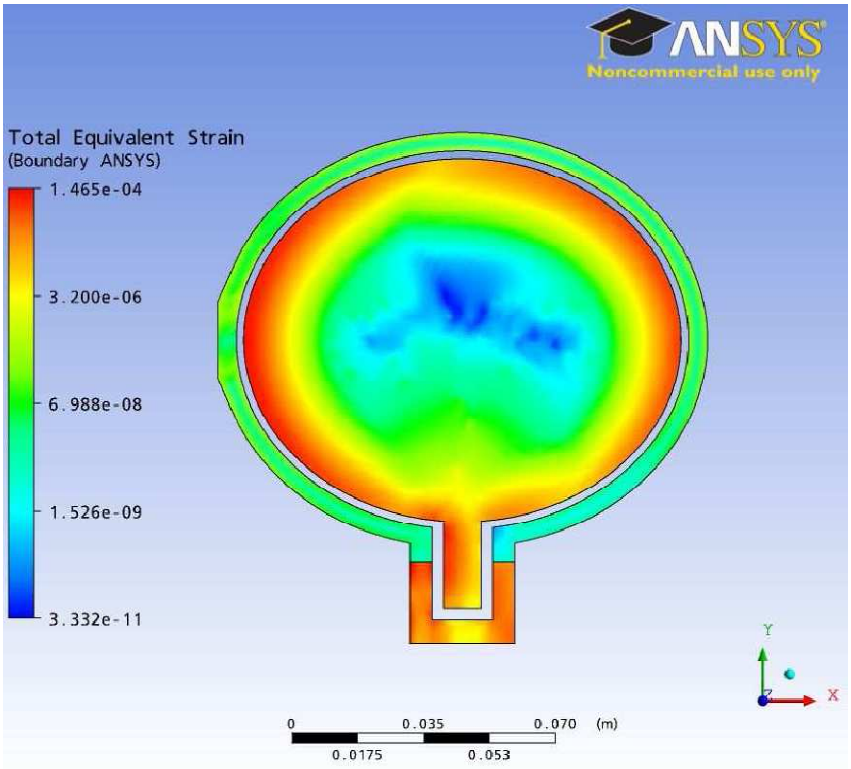

NUMERICAL SIMULATION IN TRAFFIC-RELATED BRAIN INJURIES

JAIME CABANES ARACIL
JAUME MIRO SANS

Department of applied mechanics
Division of vehicle safety
Division of fluid dynamics
Division of materials and computational mechanics
CHALMERS UNIVERSITY OF TECHNOLOGY
Göteborg, Sweden 2009

MASTER'S THESIS

NUMERICAL SIMULATION OF TRAFFIC-RELATED BRAIN INJURIES

JAUME MIRO SANS
JAIME CABANES ARACIL

Department of Applied Mechanics
Division of Fluid Dynamics
Division of material and Computational Mechanics
Division of Vehicle Safety
CHALMERS UNIVERSITY OF TECHNOLOGY
Göteborg, Sweden, 2009

Numerical simulation of traffic-related Brain injuries
Masters Thesis
Jaume Miro Sans
Jaime Cabanes Aracil

Masters Thesis

Department of Applied Mechanics
Division of Fluid Dynamics
Division of Material and Computational Mechanics
Division of Vehicle Safety
Chalmers University of Technology
Se-412 96 Göteborg, Sweden
Phone: +46-(0)31-7721400
Fax: +46-(0)31-180976

Göteborg, Sweden 2009

Jaume Miro Sans
Jaime Cabanes Aracil
Masters Thesis
by
Jaume Miro Sans
Jaime Cabanes Aracil
jaume.miro@gmail.com
jaimecabanes@gmail.com

Department of Applied Mechanics
Division of Material and Computational Mechanics
Division of Vehicle Safety
Division of Fluid Dynamics
Chalmers University of Technology

Abstract

In this thesis, it is proposed that a model of the human head is studied to investigate brain injuries. The geometry model consists of three layers of different materials, the skull, the cerebro spinal fluid (CSF) and the brain. The aim of the thesis is to try to understand the injury mechanism in a frontal impact on the head focusing on the special behavior of the CSF and its interaction with the brain. To make this possible, the computational fluid dynamics software Ansys CFX has been coupled with the finite element software called Ansys WORKBENCH. The connection between them permits the transfer of loads from the skull to the fluid and from the fluid to the brain.

In addition, several theories are proposed to explain why the brain injury is located in the frontal part (coup injury) or in the back site of the impact (contra coup injury). To model the central nervous system (CNS) different geometries and boundary conditions have been performed to simulate a more realistic pattern. However, the simplification of these models has been a difficult task due to the complexity of the organic structures and the nonlinearity of the materials, especially the brain. The lack of knowledge about mechanical properties from organic tissue such as brain tissue, was a problem during all the simulations. Previous theses have been written about mechanical brain properties but the problem remains in the differences between the tests setups. Further investigations and standardized tests are needed to get a better validation of the results.

Acknowledgment

This thesis work is performed by Jaime Cabanes Aracil and Jaume Miro Sans. It is the final part of the Master of Science program in Automotive Engineering at Chalmers University of Technology.

This thesis is the continuation of the work done by Jan Fliedner and we want to thank him for all the support and his cooperation in any moment.

We want to thank our supervisors of Applied Mechanics for their dedication, the great support during this thesis and the encouragement during the bad times: firstly, Professor Lars Davidson from the Division of Fluid Dynamics, secondly, Professor Mats Svensson from the Division of Vehicle Safety and finally, Ph.D. Håkan Johansson from the Division of Material and Computational Mechanics.

And finally, we would like to express our gratitude to our families for all the help and support.

Quería dedicar este trabajo, el cual significa la llegada a una meta tras un largo camino, a mi abuelo, mi primer gran amigo y uno de los principales responsables de que ahora sea lo que soy.

Nomenclature

Abbreviation

CSF	Cerebrospinal Fluid
CNS	Central Nervous System
TBI	Traumatic Brain Injury
FEM	Finite Element Method
EDH	Epidural Hematoma
SDH	Subdural Hematoma
ICH	Intracerebral Hematoma
DAI	Diffuse Axonal Injury
HIC	Head Injury Criteria
WSTC	Wayne State Tolerance Curve
GSI	Gadd Severity Index
HSI	Head Severity Index
ATB	Articulated Total Body
CFD	Computaional Fluid Dynamics
PMHS	Post Morten Human Subjects

Terms

ε	Strain
σ	Stress
E	Young's Modulus
ν	Poisson's ratio
Ψ	Uniaxial stress
J	Longitudinal stretch
μ_i,α_i	Material Constants
p	Pressure
ρ	Density
T	Temperature
ux	Velocity in x-direction
uy	Velocity in y-direction
∂	Derivative operator
∇	Nabla Operator
u	Velocity Tensor
t	Time
X	Dyadic Producte
τ	Stress Tensor
S_M,S_E	Source Terms
I	Unit Matrix
h	Specific Static Enthalpy
h_{tot}	Total Specific Enthalpy
λ	Conductivity
κ	Compressibility Term
V	Volume
m	Mass

p_{ref}	Reference Pressure
p_{stat}	Static Pressure
x	Displacement
a	Acceleration
v	Linear Velocity
D1	Incompressibility Parameter

Contents

1 Introduction

1.1 Epidemiology and motivation

Traumatic Brain injury (TBI) is a physical condition caused by an impact (e.g. as may be experienced in a car accident or falling from height), internal damage or loss of oxygen. The skull and the brain are suddenly subjected to an excessive amount of energy and sometimes this excess of energy may cause irreversible effects in the brain.

During the last decades a large number of statistics indicating the importance of this kind of injury have been collected. According to the Center of Neuro Skills [5], around 1.4 million of people suffer TBI each year in the United States, 500,000 die, 235,000 are hospitalized and the remaining 1,1 million receive some form of treatment. The numbers of people that suffer TBI and are not treated by emergency services are not determined.
Another study from the Center of Traumatic Brain Injury [4], from University of Pennsylvania, remarks that traumatic brain injury is the most common sort of injury.

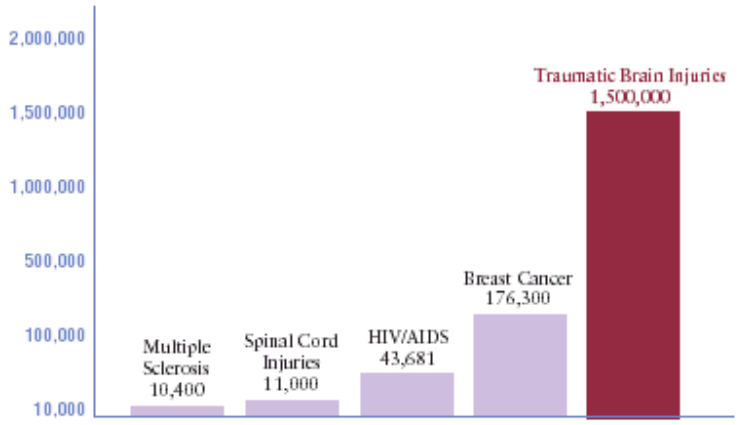

Figure 1.1 Comparison among different types of injuries, from [4].

All the information is provided by US national data which includes emergency department visits, hospitalizations and deaths. However, according to E. Finkelstein and P. Corso [8] all the data is inadequate. For instance, TBIs treated in military hospitals are not included. Neither the persons who receive medical care but TBI is not diagnosed.

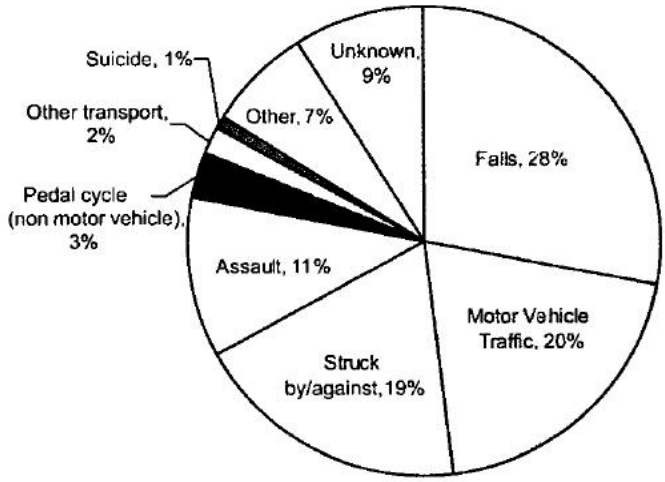

Figure 1.2 Leading causes of TBI, from [17].

The leading causes of TBI in US are falls (28%), motor vehicle crashes (20%), struck by or against items (19%) and assaults (11%), see [17]. For emergency department visits, hospitalizations and deaths, children aged 0 to 4 years and teenagers from 15 to 19 years are more likely to suffer TBI than people from other groups. Hospitalized adults aged 75 years or older are the ones with the highest risk of dying as a result TBI. As a curiosity it is pointed out that the male population is 1.5 times more likely to suffer traumatic brain injuries than females. This is due to the differences between life habits where the male population usually take more risks in their actions, see [17]
TBI can lead to long-term cognitive, behavioral and emotional consequences. D. Thurman and C. Alverson state that 5.3 million Americans, approximately 2% of the US population are living with lifelong disabilities due to TBI. Although the TBI results in a mild concussion, the long-term consequences can impair a person's abilities. In conclusion, TBI is one of the most disabling injuries [34].

Moreover, TBI can increase the risk of suffering other injuries. A recent study asserts that people who have suffered TBI are 11 times more likely to develop epilepsy than the general population for up to 3 years after their initial injury, see [31].

To try to mitigate the consequences of TBI and give a better understanding of the injury mechanism, mechanical simulations are used. FEM (Finite Element Method) is used to carry out the simulations. Actually, there are many theories about the focal brain injuries and how they are transmitted through the brain. One of the most well-known is the coup-contra-coup that results in a trauma in the rear part of the brain when an impact is applied to the front. The simulations using FEM could explain this behavior because the mechanism still remains unclear. Furthermore, it is possible to simulate impacts in brain in a transient mode where one can see how the brain deforms step by step.

Although there are still other problems that can arise like poor knowledge of brain and human tissue properties, a good understanding of the traumatic brain mechanisms would help to improve new safer devices such as proper motorcycle helmets or an improved airbag for a car.

1.2 Anatomical knowledge

1.2.1 Brain parts

The brain is the organ that mainly constitutes the central nervous system. There are numerous ways to explain the different parts of the brain. One of the most well-known approaches consists of separating the brain into subdivisions: cerebral hemispheres, diencephalon (thalamus, hypothalamus, and epithalamus), brain stem (midbrain, pons, and medulla), and cerebellum. From a technical point of view, the most interesting areas are the cerebral hemispheres. According to E.M. Marieb [20], the cerebral hemispheres account for about 83% of total brain mass.

The whole surface of the cerebral hemispheres (or also called cerebrum) is formed by an irregular shape with pronounced ridges of tissue named gyri and surrounded by channels called sulci. Moreover, the sulci separate the brain in different parts: the longitudinal fissure splits up the brain in two hemispheres, the transverse fissure separates the hemispheres from the cerebellum and the central sulcus divides the brain into the frontal lobe and parietal lobe.

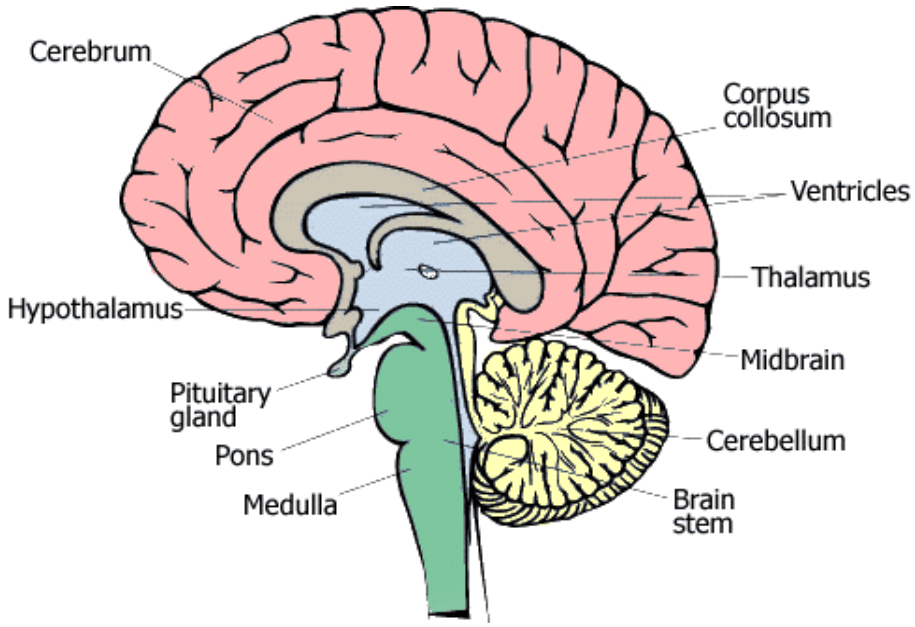

Figure 1.3 Central nervous system, from [7].

The diencephalon consists of three divisions: thalamus, hypothalamus and epithalamus. Its function is based on a switch between the central nervous and other parts. The thalamus helps to process all sensory input (except olfactory) to the cerebral cortex while the hypothalamus, is called “the brain of the brain”. It governs the homeostasis or, in other words, maintains the human body's status quo. Variables like blood pressure and heart rate are controlled by the hypothalamus, see [20].

The brain stem consists of a structure similar to the spinal cord which controls the movement and it has sensory and reflex functions. It is divided into midbrain, pons and medulla oblongata. The midbrain is in charge of processing auditory and visual systems as well as eye movement. The pons helps the information to be linked between the cerebellum and the central hemispheres. Finally the medulla oblongata has a particular role in controlling the autonomic functions like respiration, swallowing, reflexes, etc. Moreover, the medulla is the joint between the CNS and the spinal cord.

Furthermore, the brain shows three basic layers formed by different materials. The surface layer is the cerebral cortex, composed of gray matter. According to G. Francheschini [10], that layer is 2-4mm thick and contains over 50 billion neurons and 250 billion glial cells called neuroglia. Underneath, the second layer is composed of white matter, formed by axons that connect different parts of the central nervous system (CNS).

1.2.2 Meninges and skull

S. Kleiven [16] states that the meninges are made up by three layers of connective tissue: the dura mater, the arachnoid and the pia matter. However, blood vessels that enter the brain, the skull and some ventricles filled with cerebral spinal fluid are placed in meninges. The main function of meninges is to protect the brain from possible impacts, blows, shocks and friction with the skull bone. Moreover, the brain is irrigated with proteins and nutrients by the cerebral spine fluid (CSF).

First of all, the dura mater is the closest layer to the bone. It consists of a hard fibrous tissue which surrounds the inner part of the skull. It penetrates to the cranial cavity like a sheet in the tentorium cerebelli where it separates the cerebrum from the cerebellum and the falx cerebri dividing the brain into two hemispheres.

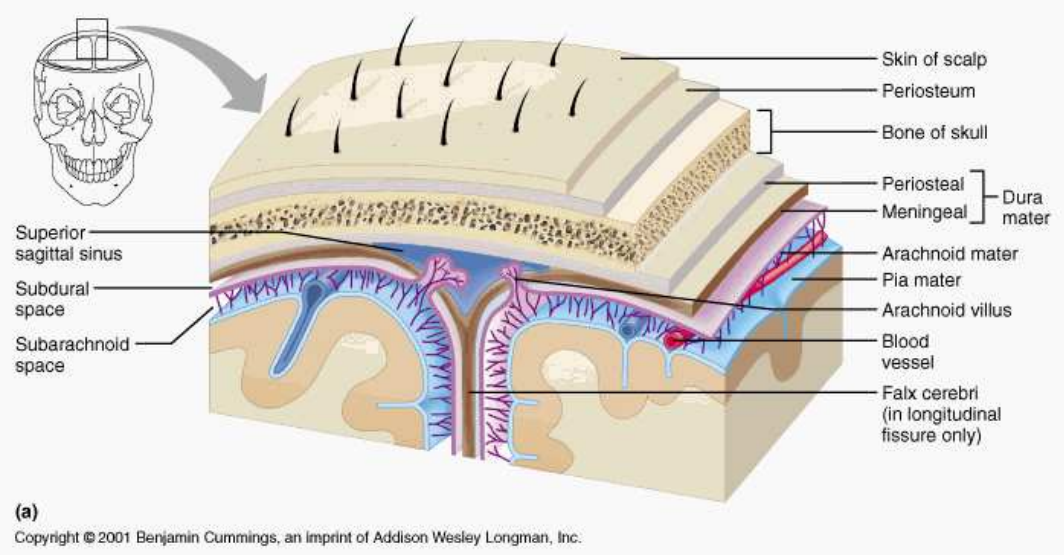

Figure 1.4 Meningeal layers, from [20].

The “spider web” called arachnoid is located below the dura mater. It is full of blood vessels and resembles a web, hence its name. Although it never dips into the brain sulci, it surrounds the spinal cord and the inner part of the dura. Beneath this membrane, the subaachnoid space is placed filled with cerebrospinal fluid (CSF). The liquid encloses and protects the brain like a cushion against the shocks. Moreover, there are filaments called arachnoid trabeculations that link the arachnoid to the pia to reduce the relative movement between both parts. Thus, the brain is protected from Shear Stress mostly caused by rotational displacement, see [16].

Finally, the pia mater is located above the cerebral cortex and is completely attached to the brain surface. It is a meningeal layer composed of fibrous tissue and impermeable to the fluids as well, see [3].

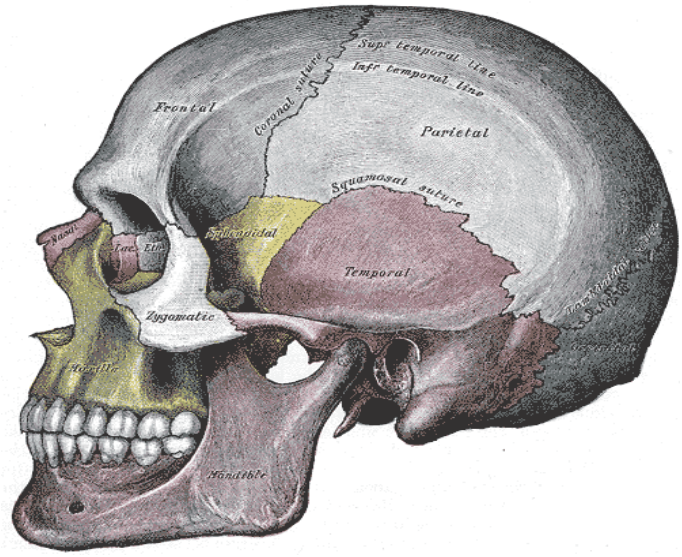

Figure 1.5 Skull and face bones, from [6].

The skull is the most external barrier that protects the brain. It fulfills a remarkable compromise between weight and strength, it helps to fix the distance between the eyes and it fixes the position of the ears improving the sensitivity and accuracy of the brain.

1.2.3 Cerebro spinal fluid (CSF)

The subarachnoid space is the gap between the pia mater and the ventricles of the brain. It is produced in the lateral ventricles which are located in the left and right hemisphere and linked under the corpus callosum. The fluid flows from these two ventricles to the third one and from there to the fourth through a channel that also is connected to the spinal cord. These ventricles, also described as caverns, are sometimes opened to the subarachnoid space. For instance, there is an opening at the rear of the third ventricle where the liquid can flow through the sulcus placed between the cerebellum and the cerebrum.

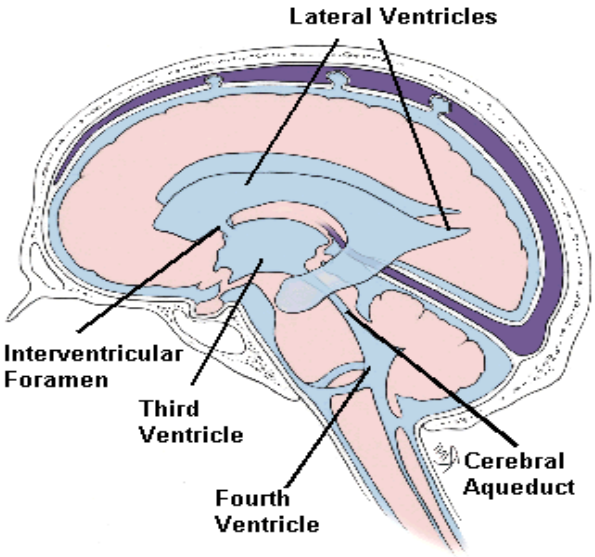

Figure 1.6 Brain ventricles filled with CSF, from [24].

Mainly, the cerebro spinal fluid encircles the brain and the spine being responsible for transporting the nutrients and cushioning the brain from mechanical shock. In the arachnoid granulations the drainage of CSF is stored, and the majority of the liquid is returned. According to Franceschini [10], in an adult, approximately 140 ml of CSF surrounds the brain. It also states that for normal movements the inner pressure (and any shrinkage or expansion) of the brain is counter-balanced by an increase or decrease of cerebro spinal fluid.

1.3 State of the art

1.3.1 Brain injury mechanisms

To describe the mechanisms that lead to brain injuries many models have been developed. The most common are notional and experimental models. The first ones are derived by the analysis of the damaged and torn tissue while the others are based on the empiricism of the experiments. With the experiments, one can observe how the combination of the loads and shear stress produces deformation in the tissues and, thus, injuries. Although all of them note a general understanding of the problem, they cannot explain the mechanism.
From the medical literature, it has been found that the injury theories have been developed long ago and nowadays the brain injuries are mainly separated in two groups: focal injuries and diffuse injuries. The focal ones cause damage in a specific area and they can be identified with the naked eye, while the others are associated with a general break of brain tissue or disruption of neurologic function and are not related to macroscopic brain lesions. Generally, in the diffuse injuries, the damage is due to the acceleration in the tissue. Basically, the focal injuries are epidural hematomas (EDH), subdural hematomas (SDH), intracerebral hematomas (ICH), and contusions (coup and contrecoup). The diffuse injuries are brain swelling, diffuse axonal injury (DAI) and concussion. [33]

G.M. McHenry [22] states that there are two more ways to classify brain injuries. The first one relates to the cause of the injury, such us contact or non-contact. The second distinguishes between types of injury: primary and secondary injuries. The primary injury occurs when the initial injury is produced. On the other hand, the secondary injury does not appear until sometime later.

1.3.1.1 Focal injuries [16]

Subdural hematoma (SDH)

Subdural hematomas are caused by the tearing of arteries located in the inner meningeal layer of the dura and those that link the arachnoid mater with the dura mater.

Epidural hematoma (EDH)

EDH consists of blood gathered between the skull and the outer meningeal part of the dura. Moreover, it can increase the intracranial pressure and, thus, induce damages in the brain tissue.

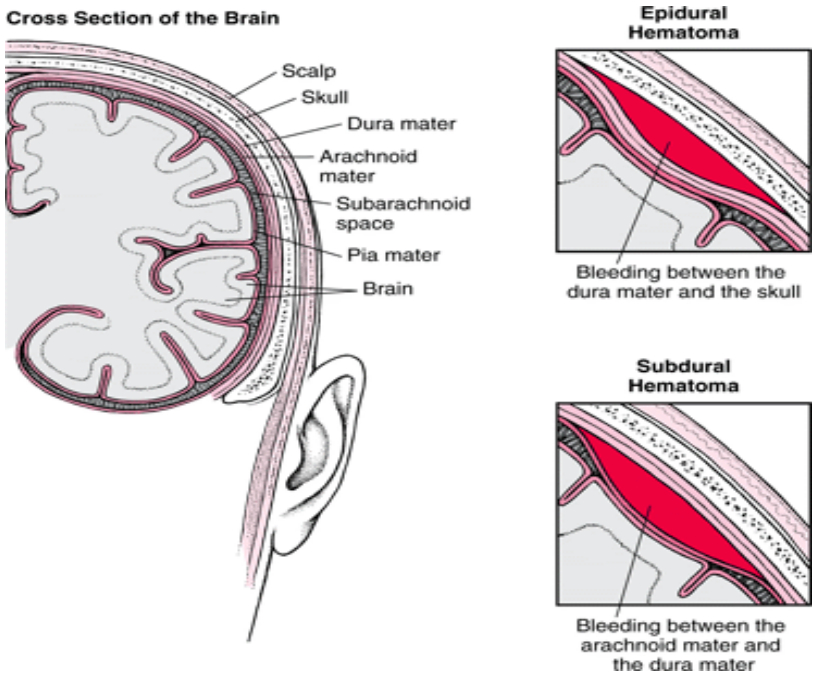

Figure 1.7 Epidural and subdural hematoma (pocket of blood), from[25].

Contusions

Contusions are created by bruises inside the brain caused crashes and blows to the head. Contusions may be created by sudden deceleration of the brain when the head strikes an immobile object in the middle of the path (frontal-impact motor crash accident). Contusions

can occur on the site of the impact (coup contusions) or on the opposite side of the site of impact (contrecoup contusions).

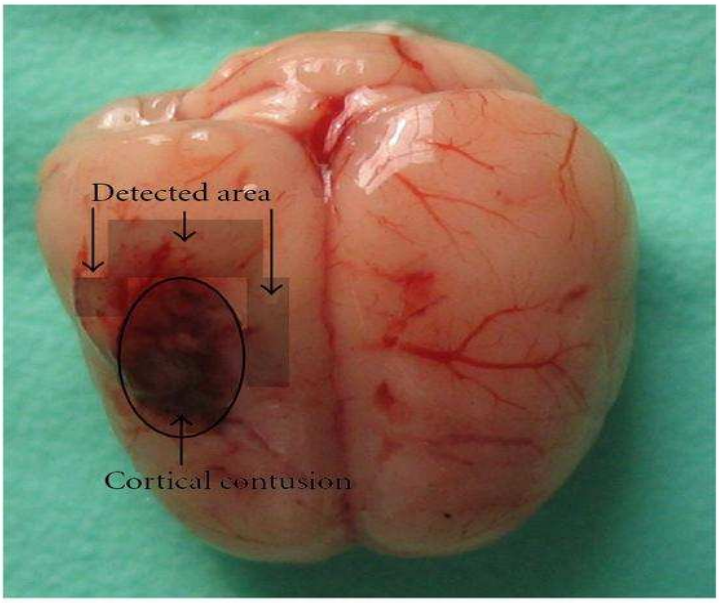

Figure 1.8 Schematic representation of the cortical contusion area induced by weight-dropping trauma and the studied region surrounding the injured brain, from [13].

Intracerebral hematomas (ICH)

ICH consists of accumulations of blood within the brain. This blood can compress the brain and sometimes surgery is needed to reduce the intracranial pressure.

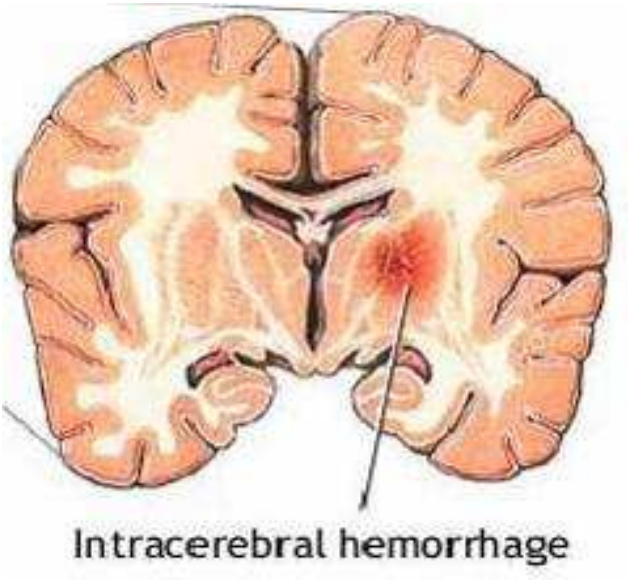

Figure 1.9 Intracerebral hematoma, from [6].

1.3.1.2 Diffuse injuries

Concussions

Concussions are also called mild traumatic brain functions. They can be defined as a short period where the patient loses the consciousness due to a head trauma (see fig 1.10). The brain function can be interrupted but there is no permanent damage. In general, 95% of the patients have a good recovery after one month.

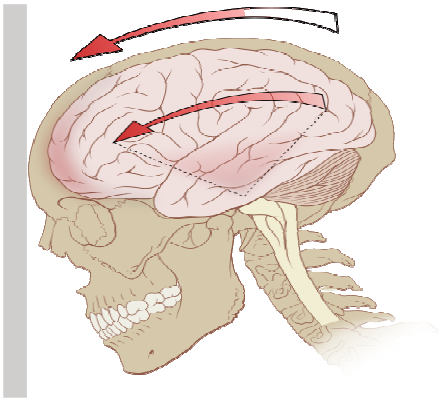

Figure 1.10 Head trauma caused by a frontal impact, from [12].

Diffuse axonal injuries (DAI)

DAI denotes a widespread injury in axons and nerve cells. It usually occurs due to acceleration/deceleration of the head as can occur in traffic accidents. The mechanism consists in the disruption of the axons and thus, their neural function that permits neurons to communicate between them. Diffuse axonal injury typically causes loss of consciousness that lasts for more than 6 hours. Sometimes the person has symptoms of damage to a specific area of the brain. Increased pressure within the skull may cause coma.

Brain swelling

Brain swelling is also named edema. It corresponds to an increase of the blood inside the brain which can cause an increase in intracranial pressure, preventing blood from entering the skull to supply oxygen and glucose to the brain.

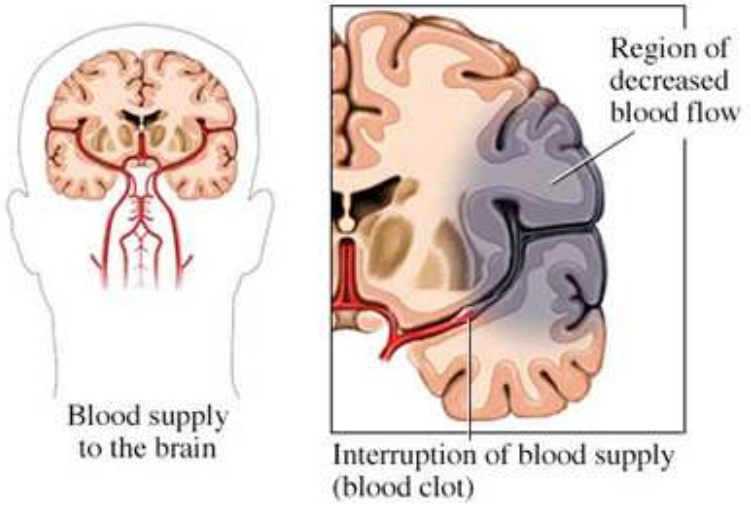

Figure 1.11 Blood clot has interrupted the blood supply to the brain, from [2].

1.3.1.3 Head Injury Criteria (HIC)

The HIC is a method to predict head injuries following impact with flat objects, taking into account the deformation of the skull and the brain injuries including the possible loss of consciousness. The basis of this approach lies in the medical background that states that 80% of patients with linear skull fractures show concussions [16]**.** It is calculated with the translational acceleration of the head.

$$HIC = \left\{ (t_2 - t_1) \left[\frac{1}{t_2 - t_1} \int_{t_1}^{t_2} a(t)dt \right]^{2.5} \right\} \quad \text{Eq 1.1 [16]}$$

Its major drawback is the inconsistency that appears when a severe brain injury may not be related to a large skull fracture.
HIC was a curve fit to the Wayne State Tolerance Curve (WSTC) at the beginning. WSTC denotes a relationship between acceleration level and impulse duration concerning head injury. First, it only covered time duration of 1 to 6 milliseconds and later was complemented with animal, cadaver and volunteer data. However, the curve has some limitations such as reduced number of data points, or none cleared scaling of animal data and uncertain acceleration levels.
Brian G. Mc Henry states that the main inconvenience of the WTSC is the biomechanical parameters because it is not possible to prove direct functional brain damage when an injury mechanism is determined. [22]

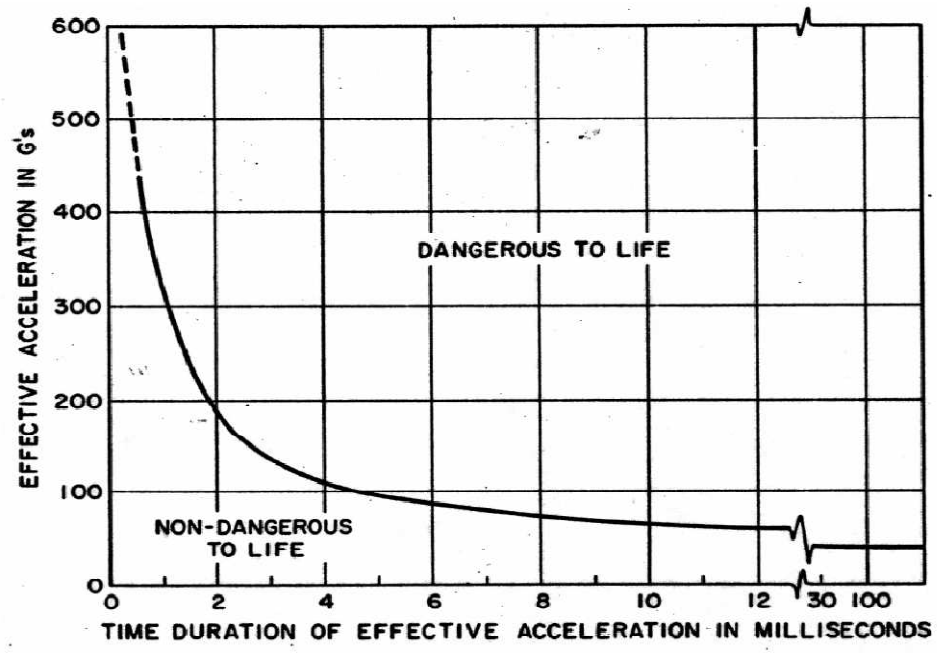

Figure 1.12 Wayne State Tolerance Curves, from [6].

C.W. Gadd [11] plotted the WSTC data in a logarithmic law and that criterion became known as the Gadd Severity Index (GSI). Another indicator is the HSI which is the same as GSI but is the one included in the Articulated Total Body model. The ATB is a computer code which is used for dynamic motion simulations of jointed systems of rigid bodies.

$$HSI = \int [a(t)]^{2.5} dt \qquad \text{Eq 1.2 [11]}$$

1.3.2 Experiments

Nowadays with the help of FEM and CFD software and the ever-increasing speed of computational time, the simulations have gained importance. However, they should always be compared with “the real world”. One of the aims of the experiments in biomechanic fields is to try to validate the results that are released from the simulations. The experiments can be focused either in enriching the material theories and properties or improving the comprehension of the injury mechanisms. Furthermore, the research and development in biomechanics can be split up in four categories:

Post mortem human subjects (PMHS): Corpses are usually used for testing to failure. The limitation appears with tissue properties that are softer than the ones from living humans and it is impossible to release a physiological response. In these experiments isolated body segments like heads, arms and necks are tested instead of collecting material data.

Animal models: They are subdivided in two subgroups. First of all, small animals like rats, mice and rabbits are used to improve the knowledge of the tissue properties and physiological responses. Secondly, larger mammals such us apes and monkeys are tested because they are more similar to humans in terms of brain mass.

Volunteers: They consist of living humans submitted to testing. The main drawback is the absence of injury that must be a requirement. However, they are useful for understanding body kinematics.

Specimen or cultivated cells: Some cells and tissue parts are tested and analyzed. Generally these experiments are made with the purpose of improving the knowledge of material properties.

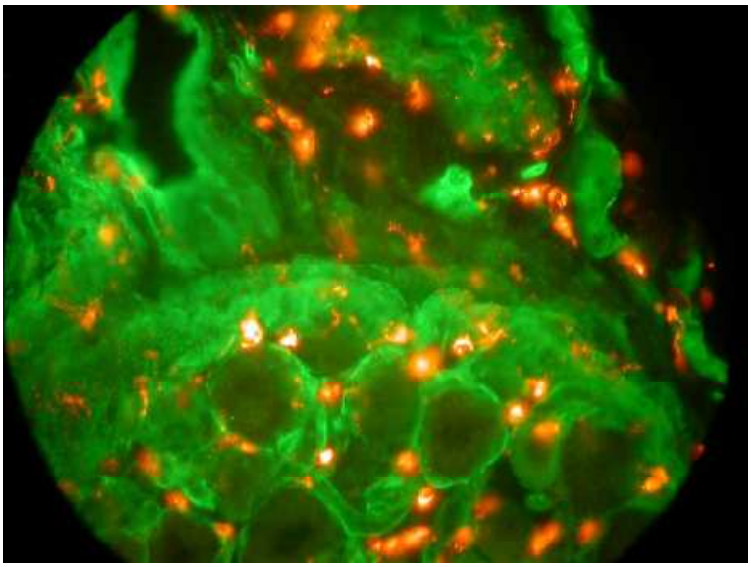

Figure 1.13 Tissue analysis, from [6].

In the experiments with animals, where the investigations are focused on big parts of the body, the scenario usually remains the same (e.g. frontal or lateral impact to the head) but the rigs and the setup differ from one experiment to another. This lack of standardization and information makes the tests difficult to compare and it is arduous to obtain conclusions, see [28].
An example of in vivo experiment can be found in D. F. Meaney and A. C. Bain [23]. The tests consisted of stretching optic nerves of an adult male guinea pig. In fact, the optic nerves are made of myelinated nervous fibers which coincide with brain tissue from white matter. The aim of [23] is to prove that tissue strain is a good parameter to determine the level of axonal injury. Subsequently, they provided strain-based thresholds for damage in white matter. However, a limitation found in this thesis may be the microstructural arrangement of the axon nerves within the tissue. In the guinea pig´s optic nerve the axons were waved and when the load was applied they reorganized, forming a whole fibrous and isotropic material.

This may differ from the typical white matter structure from the cerebrum which is not usually isotropic. Although it is the first study that states thresholds for strain in CNS, it may not be suitable for using the strain rate in human head model. Thus, an absence of experiments should be added to the lack of information that has been mentioned before.

1.3.3 Material theories

Trying to find the best materials is one of the most challenging tasks in this project, although the material theories for the skull and cerebrospinal fluid (CSF) are very simple. There is plenty of research about the properties of skull bones that have been tested with human bodies due to the bones properties keep constant even when the body is dead. Analyzing this data one can conclude basically that the skull behaves as an isotropic material and can be modeled with a linear elasticity theory. Regarding the CSF, its properties are water-like. On the other hand, the brain demands considerably more work; it is a very uncommon material with very special properties. It is worth analyzing the characteristics that make the brain such a special material.
The brain is a heterogeneous system and its mechanical model is affected by the following components: the tissue, whose mechanical characteristics are determined by the corresponding features of the membranes of the cell elements, the blood, which affects the mechanical properties through changes in the volume of blood cerebral vessels and in the intra vascular pressure level. Taking into account these effects it is easy to understand why most of the methods used with dead specimens are prevented from being adequately investigated. So far some research in vivo has been published that is vital for understanding certain physiological and pathological processes. [14]

The mechanical properties of the brain are a consequence of under uniaxial (quasi-static), cyclic loading, brain tissue exhibits a peculiar nonlinear mechanical behavior, exhibiting hysteresis, Mullins effect and residual strain, qualitatively similar to that observed in filled elastomers. Brain tissue should, therefore, be modeled as a porous, fluid-saturated, nonlinear solid with very small volumetric (drained) compressibility [10].

The hyper-elastic models such as Ogden nonlinear elastic theory or Mooney-Rivlin are able to represent the nonlinear properties as well as the incompressibility, but there is something else that these theories are not able to model, the time dependence. Some quasi-static experiments have been made with very successful results but since a traumatic brain injury often occurs in dynamic conditions the results are still unsatisfactory. In fact, nowadays, there is not a clear idea how the brain should be regarded because there are polemic debates about its compressibility (whether it is compressible or just capable of isochoric deformation). There are doubts about which theory is more suitable; the linear model or nonlinear theory with or without anisotropy, even if it has viscoelastic behavior or if it exhibits permanent deformations. Thus, a perfect model has not been created yet and it always depends on the type of experiment. [26][27][15]

1.3.4 Numerical Method

In order to solve the problems presented by the continuum mechanics, the engineer has to deal with solid mechanics and fluid mechanics. Over the last 30 years, many scientists have tried to model the head. The skull has not been a very controversial problem to build due to its dominant elastic properties. On the other hand the brain and the skull-brain interface, where the CSF is located, have had different approaches, but the lack of a powerful tool to successfully solve the coexistence between the solid parts (skull, brain) and the liquid part (CSF) have resulted in an absence of information. These problems are solved by CFD analysis, which involves fluid flow, heat transfer and associated phenomena such as chemical reactions by means of computer-based simulation. The technique is very powerful and spans a wide range of industrial and non-industrial application areas. Even though the Computational Fluid dynamics was used more than 40 years ago (Paul Rubbert and Gary Saarys of Boeing -Aircraft, 1968; NASA PMARC) this tool required a very powerful computer in order to solve the most basic 3D fluid problems. Nowadays there is a wide range of commercial software that is based on CFD problems. In this thesis, Ansys Workbench is the software used to solve the solid-liquid interaction.

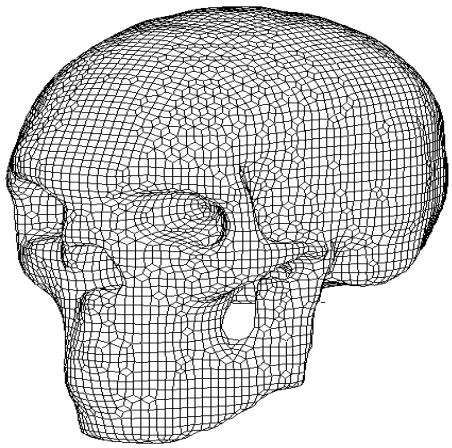

Figure 1.14 3D skull model created by Gerald Krabber and Ralph Muller

Due to the cost of the experiments, this sort of mathematical algorithm has been used to simulate brain and head injuries. There are many advantages to this method such as the possibility of recreating a suitable scenario for each situation, the possibility of using different materials and so on but the main one is the low cost of the simulations compared to the real experiments. On the other hand, the drawbacks are the lack of accuracy and the need for validation. It is usual to work with both methods, first work with FEM and then test the results with real experiments. Nowadays, there is a wide range of FEM software; in this project ANSYS Workbench has been chosen. This software has mainly 3 parts:

The pre-processor: where the geometry and the mesh are created.
The processor: in this step the problem scenario is defined (loads, boundary conditions) and

the software solves the problem.
The Post-processor: where the solution can be analyzed and all the data can be extracted.

So far many models have been created in order to study the behavior of the head in a crash impact; the first one was modeled by Anzelius in 1943. He designed a spherical liquid mass and he focused on the pressure which caused the coup-contrecoup effect due to the acceleration.
The first 3D models were very simple as well, with geometries such as spherical (Chan, 1974), spheroidal (Kenner and Goldsmith, 1972) and ellipsoidal (Hubbard, 1977). Moreover, there are other early works with very realistic skull shape (Hardy and Marcal, 1973; Hosey and Liu, 1981; Nickell and Marcal, 1974; Shugar, 1975, Ward, 1982). All these models, apart from Hosey and Liu (1981) considered just one of the major parts of the head: the skull or the brain.
It is in the 1990s when the major parts of the head are included together in the model (Ueon, 1995; Cheng, 1990; Ruan, 1994 and 1997; Zhou, 1995 and 1996; Willinguer, 1995 and 1999), that is just an example of the amount of models that have been created, different brain properties were tested such as linear elastic or viscoelastic with the aim of solving the problem of the skull-brain interfaces in different ways. Due to the lack of technology to develop a solid-fluid interaction, they used a solid CSF or other types of solution more or less accurate. It was in 2002 when S. Kleiven created a model which was composed with brain, skull and CSF as a water material. It was an important step forward for understanding the mechanism of the head injury, since this experiment made it possible to investigate the wave propagation of the fluid and check effects such as cavitation or shear stress. [16]

In this task the same goal wants to be achieved. Ansys Workbench allows working with CFD and FEM to obtain more realistic results; it is noteworthy to have an idea of how this software works to understand the complexity of the simulation. The configuration of the scenario influences the difficulty of the simulation. There are two solid bodies which can shift in three degrees of freedom and only interacting by fluid-solid interfaces being coupled with two different numerical solvers - but this is not a real coupling. The solvers only exchange their results, and adjust them to each other. So information has to pass from each solver twice in order to obtain the information from the skull to the brain. That causes a high instability because sometimes the equations used are not possible to solve. Even though the software is not fully prepared for this sort of problem the possibility of working with FEM and CFD simultaneously is one of the challenges in this project.

1.4 Scope of the investigation

The scope is to discover the effects of a frontal impact, that is, linear acceleration would be applied to the front of the head, and the head would be formed by three different parts, the brain, the CSF and the skull. The coup-contrecoup effect is expected so the post-processing would consist of studying the causes of such effect. To discover them, there are phenomena which have to be analyzed such as the wave propagation, the changes in the liquid pressure and the influence of different stiffness of the skull.

2 Methodology

2.1 Theoretical model

Two different numerical methods are used in order to reach the goal of this thesis: Finite Element Method (FEM) and Computational Fluid Dynamics (CFD). The first numerical method (FEM) is in charge of solving the solid part of the problem (skull, Brain), while the CFD would solve the liquid part (CSF).

2.1.1 Finite Element Model

2.1.1.1 Elastic Theory and governing equations [30][29][18][19]

It is important to describe the behavior of the solid materials that are used. In this project the skull is presented as a linear elastic material. The first assumption that is made is that the body is homogeneous and continuously distributed over its volume. To simplify it, one can state that the body is isotropic, that is, the elastic properties are the same in all directions.

There are two components of interest: the stress and the strain. The stress is a measure of the average amount of force exerted per unit of surface area where internal forces act within a deformable body. It is the measure of the intensity, or internal distribution of the total internal forces acting within a deformable body across surfaces. On the other hand, the strain is the geometrical measure of the deformation representing the relative displacement between particles in the material body.

The governing equations in the FEM software (ANSYS) for the elastic materials are as follows:

Equation of motion

The equation of motion is an expression of Newton's Second law.

$$\nabla \cdot \sigma + f = \rho \ddot{u} \qquad \text{Eq. 2.1}$$

Where σ is the Cauchy stress, f is the volumetric body force, ρ is the density and ü is the acceleration.

Strain-displacement equations

The relation between strain and displacement in a matrix format is:

$$\varepsilon = \frac{1}{2}\left[\nabla u + (\nabla u)^T\right] \qquad \text{Eq. 2.2}$$

Where ε is the strain and u is the displacement.

Constitutive equations

The general strain-stress relationship has been established experimentally and is known as Hooke's Law:

$$\sigma = c : \varepsilon \qquad \text{Eq. 2.3}$$

Expressed in terms of components with respect to an orthonormal basis, the generalized form of Hooke's law is written as:

$$\sigma_{ij} = c_{ijkl}\varepsilon_{kl} \qquad \text{Eq 2.4}$$

In a three-dimensional stress state, the 4th order tensor c called stiffness tensor containing 81 elastic coefficients links the stress tensor σ with the strain tensor ε.

Elastic model has been chosen in order to model the skull bones, because it is a precise approximation in this case. [32]

The other parameter that has been established experimentally is the Poisson's ratio *v.* It is the ratio of the contraction or transverse strain. [32]

2.1.1.2 Hyper-elastic theory and governing equations [33][29][18][19]

More sophisticated elastic models are required for organic materials like the brain. It exhibits a nonlinear stress-strain behavior even at modest strains. This material shows complex nonlinear stress-strain behavior. Specific strain energy-functions are designed to account for these phenomena.

Ogden´s model has been chosen due to research made by Giulia Franceschini [9] who established that the brain is shown to behave qualitatively similar to filled elastomers and is, therefore, shown to follow the Ogden (1972) constitutive theory. However the porosity of the brain has to be taken into account, but since the model has been simplified the hyper-elastic theory fulfills the main requirements.
According to Ansys data [1], when the material is hyper-elastic the software reports the stresses as the 2nd Piola-Kirchoff stress tensor, s, and the strain as the Lagrangian strain tensor, E. Thus, the governing equations are:

Equation of motion

The equation of motion remains the same but the stresses are reported according to 2nd Piola-Kirchoff, which is obtained by expressing components of traction force on each surface of the deformed material element in terms of the base vectors of the deformed triad $(\bar{i}, \bar{j}, \bar{k})$.

$$\nabla\sigma + f = \rho\ddot{u} \qquad \text{Eq. 2.5}$$

$$S = J F^{-1} \sigma F^{-T} \quad \text{Eq. 2.6}$$

Where S is the 2nd Piola-Kirchoff stress tensor, F is the deformation gradient, $J = \det F$ is the Jacobian determinant and σ is the Cauchy stress tensor.

Strain-displacement equations

The deformation tensor called right Cauchy-Green tensor is defined as:

$$C = F^T F \quad \text{Eq. 2.7}$$

Where C is the Cauchy-Green deformation tensor, F is the deformation gradient.

The Lagrangian strain tensor is related to C as:

$$C = 2E + 1 \quad \text{Eq. 2.8}$$

Constitutive equations

The constitutive equations of the hyperelastic theory are defined in terms of an internal energy ψ, expressed in terms of the left Cauchy-Green tensor (C).

$$\Psi(C) = \Psi_{vol}(J) + \Psi_{iso}(\overline{C}) \quad \text{Eq. 2.9}$$

Where the ψ was split into a volumetric and an isochoric part.

$$\overline{C} = J^{-2/3} C \quad \text{Eq. 2.10}$$

$$\overline{\lambda_i} = J^{-1/3} \lambda_i \quad \text{Eq. 2.11}$$

The 2nd Piola-Kirchoff stress is given in terms of internal energy.

$$S = \frac{\partial \psi}{\partial C} \quad \text{Eq. 2.12}$$

The isochoric part of the strain energy is given according to Ogden's model in terms of the longitudinal stretch $\overline{\lambda}$:

$$\Psi_{vol}(\overline{\lambda}_1, \overline{\lambda}_2, \overline{\lambda}_3) = \sum_{P=1}^{N} \frac{\mu_P}{\alpha_P} (\overline{\lambda}_1^{\alpha_P} + \overline{\lambda}_2^{\alpha_P} + \overline{\lambda}_3^{\alpha_P} - 3) \quad \text{Eq. 2.13}$$

Where α_P and μ_P are constitutive parameters. They are related to the initial shear modulus as:

$$\mu = \sum_{k=1}^{N} \alpha_k \mu_k \quad \text{Eq 2.14}$$

ANSYS uses for all hyper-elastic and the volumetric part of the strain energy:

$$\Psi_{vol}(J) = \sum_{i=1}^{M} \frac{1}{d_{ik}} (J-1)^{2i} \quad \text{Eq 2.15}$$

If M=1, d1=2/K, where K is the Bulk modulus

[33][36]

2.1.2 Computational Fluid Dynamics

The brain fluid remains almost in a static state, that is, it has to be treated as a laminar fluid due to its low Reynolds number. It is necessary to study the behavior of the liquid during the whole experiment. Another factor to take into account is the different cavities where CSF can flow such as inside and outside the brain and through the spinal cord but the volume compensation of the CSF has been considered as being of minor importance. In order to simplify the problem and according to M. Y. Svensson [31] it can be assumed that there is no penetration of the liquid through the brain and just a slight expansion of the spinal cord whether the fluid compresses or not. The CFD used in this project is based on finite volume method which is in fact very similar to the finite element method. CFD is based on Navier-Stokes equations, which govern the algorithm and they are solved numerically through iterative methods and it is not possible to find the exact solution. However, a good and trustworthy solution can be achieved. Navier-stokes equations are responsible for dealing with the conservation of mass energy and momentum. There are many types of algorithm; they differ in speed of calculation, accuracy and stability, depending on the order of the algorithm. If the algorithm is second order accurate like for example Second-Order Upwind scheme the error is reduced by a number of four when the number of cells are doubled. That makes remarkable differences between schemes even though there are more important factors to take into account like the stability of the scheme. In this case the scheme followed is the high resolution scheme. This sort of strategy is very accurate, more than the upwind scheme but not that stable. More aspects worth paying attention to include the residuals, time step selection or the number of stagger iterations. The number of iterations that the algorithm has to do before it changes the time step either has converged or not. It is impossible to know which configuration is best for most of these, so the experience plays an important role when a CFD simulation is running.

2.1.2.1 Governing equations for the fluid [35]

The governing equations of fluid flow represent mathematical statements of the conservation laws of physics. The fluid is defined by the following variables: pressure p (Pa), the density ρ (kg/m^3), the temperature T (ºC) and the velocity u (m/s^2). Each cell of the mesh is defined by them and depending on the geometry dimensions; the number of variables would be different. In this case, 2D, the number of variables are 5 (p, ρ, T, ux, uy) where ux and uy are the velocity components in x and y axis respectively.

The governing equations manage to conserve the mass of fluid, the momentum change rate equals the sum of the forces on a fluid particle (Newton's second law) and the energy variation rate is equal to the sum of the heat and the work done on a fluid particle (first thermodynamics law).

The fluid will be regarded as a continuum. For the analysis of fluid flows several different forms for the equation are available, in this project conservative Navier Stokes equations for continuity and momentum have been used.

Mass conservation

The first step is to establish the mass balance for the fluid element:
The rate of mass incrementation in fluid element equals the net variation of mass flow into fluid element

$$\frac{\partial \rho}{\partial t} + \nabla \cdot (\rho u) = 0 \qquad \text{Eq 2.16}$$

The first term is the rate of change in time of the density (mass per unit volume). The second term describes the net flow mass out of the element across its boundaries and is called the convective term,

The equation (1) is the unsteady, three-dimensional mass conservation or continuity equation at a point in a compressible fluid.

Momentum equation

According to Newton's second law the momentum of a fluid particle equals the sum of the forces on the particle. The balance would be: increasing the momentum of fluid particle is equal to the sum of forces on the fluid particle.

$$\frac{\partial(\rho u)}{\partial t} + \nabla \cdot (\rho u \otimes u) = -\nabla p + \nabla \tau + S_M \qquad \text{Eq 2.17}$$

It can be distinguished two types of forces on fluid particles, the surface forces (pressure, viscous and gravity) and the body forces (centrifugal, Coriolis).

The stress tensor τ can be related to the strain rate by the following expression:

$$\tau = \mu(\nabla u + (\nabla u)^T - \frac{2}{3} I \nabla \cdot u) \qquad \text{Eq 2.18}$$

Energy equation

The specific energy E of a fluid is defined as the sum of internal energy, kinetic energy and gravitational potential energy

$$\frac{\partial(\rho h_{tot)}}{\partial t} - \frac{\partial p}{\partial t} + \nabla \cdot (\rho u h_{tot}) = \nabla(\lambda \nabla T) + \nabla(u\tau) + u \cdot S_M + S_E \quad \text{Eq. 2.19}$$

In Eq. 2.19 we have $h_{tot} = h + \frac{uu}{2}$ Eq. 2.20

It describes the total specific enthalpy which is related to the static enthalpy (p, T).

2.2 Coupling Ansys CFX to Ansys solver [34]

This simulation requires the coupling of the CFX solver to Ansys Solver. Coupled simulations follow a timestep/iteration structure. During coupled simulations, the CFX and the Ansys solver execute the simulation through a sequence of multi field timesteps, each of which consists of one or more "stagger" iterations. During every stagger iteration, each field solver gathers the data it requires from the other solver, and solves its field equations for the current multi-field timestep. Stagger iterations are repeated until a maximum number of stagger iterations is reached or until the data transferred between solvers and all field equations have converged. The latter guarantees an implicit solution of all solution fields for each multi-field timestep. The MFX solver is a version of the ANSYS Multi-field solver which allows the coupling of ANSYS CFX with ANSYS Mechanical or Multiphysics. It allows the performance of simulations where it is necessary to couple the fluid physics and solid physics throughout the solution process, rather than just by passing data from one solver to the other at the end of the simulation. The ANSYS Multi-field set-up requires the set-up of the fluid physics in CFX, set-up of the solid physics for ANSYS, and the specification of the MFX coupling settings.

In ANSYS Multi-field solver, data is communicated between the ANSYS CFX and ANSYS field solvers through standard Internet sockets using a custom client-server communication protocol. Setup requires creation of the fluid and solid domain/physical models in the ANSYS CFX-Pre and ANSYS user interfaces, respectively, and the specification of coupling data transfers and controls in the ANSYS CFX-Pre user interface. Execution and run-time monitoring of the coupled simulation is performed from the ANSYS CFX-Solver Manager.

It must be specified an ANSYS input file which contains the ANSYS setup for the MFX problem, including the identification of the Fluid Solid Interfaces on the ANSYS model. This will be used by ANSYS CFX-Pre to determine the valid interfaces for selection later on, and will also be used by default as the ANSYS input file when the solver run is started from ANSYS CFX-Solver Manager.

Coupled simulations begin with the execution of the ANSYS and CFX field solvers. The ANSYS solver acts as a coupling master process to which the CFX solver connects. Once that connection is established, the solvers advance through a sequence of six pre-defined synchronization points (SPs), as illustrated in Figure 2.1. At each of these SPs, each field solver gathers the data it requires from the other solver in order to advance to the next point.

The first three SPs are used to prepare the solvers for the calculation intensive solution process, which takes place during the final three SPs. These final SPs define a sequence of coupling steps, each of which consists of one or more stagger/coupling iterations. During every stagger iteration, each field solver gathers the data it requires from the other solver, and solves its field equations for the current coupling step. Stagger iterations are repeated until a maximum number of stagger iterations is reached or until the data transferred between solvers and all field equations have converged. The latter guarantees an implicit solution of all fields for each coupling step.

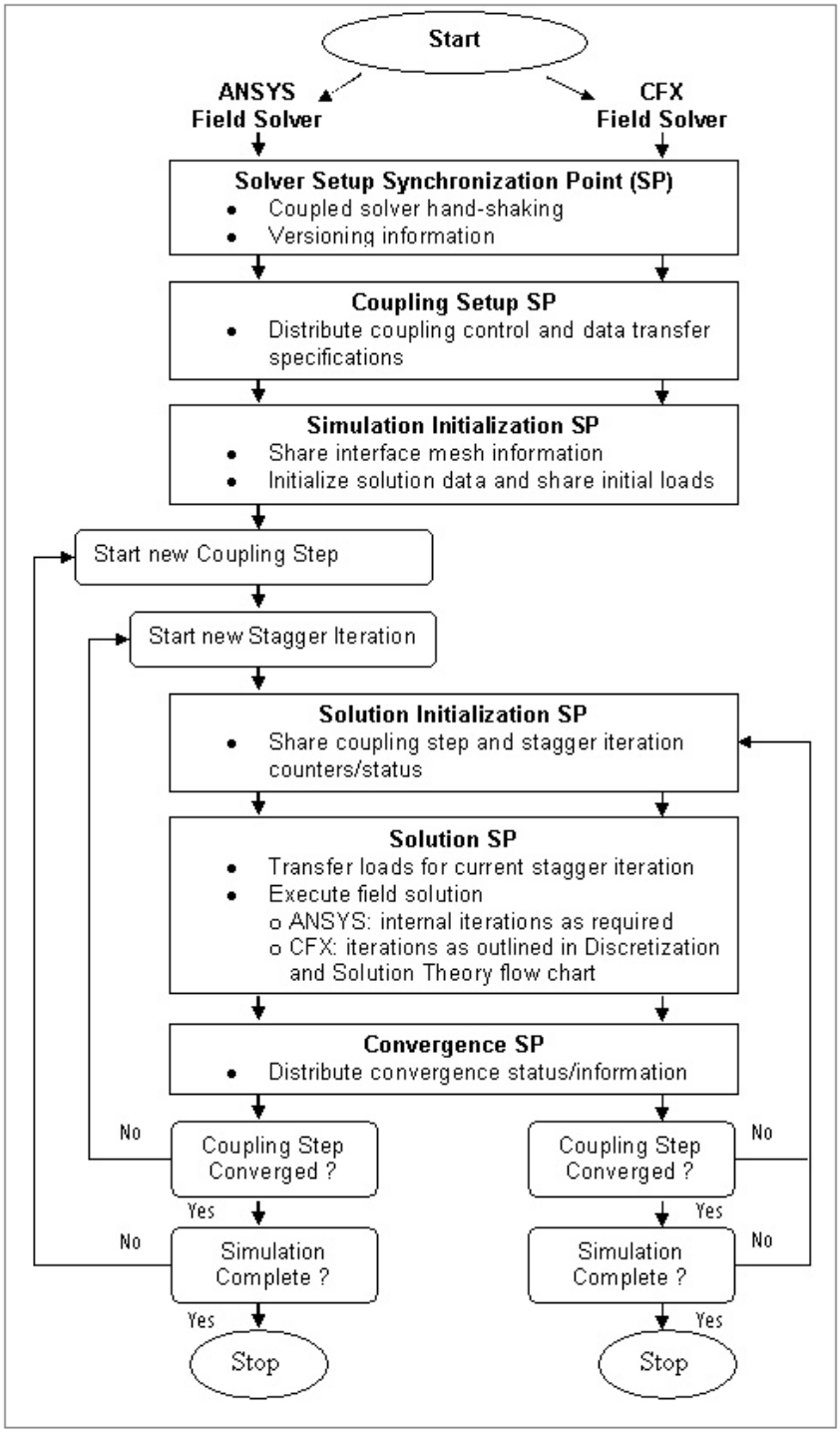

Figure 2.1 Coupling method diagram

3 2D Models

3.1 Geometry

In order to create the model, first of all the geometry has to be built. For that task the ANSYS WORKBENCH design modeler is used and the geometry consists of three parts, two solids and one liquid. The solid parts are the brain, the skull and the neck, and they are built independently of the liquid part due to the fact that they need a different mesh strategy to the CSF, because the manner in which a CFD solves its problems is different to the way that the FEM does, in spite of its similar procedure.

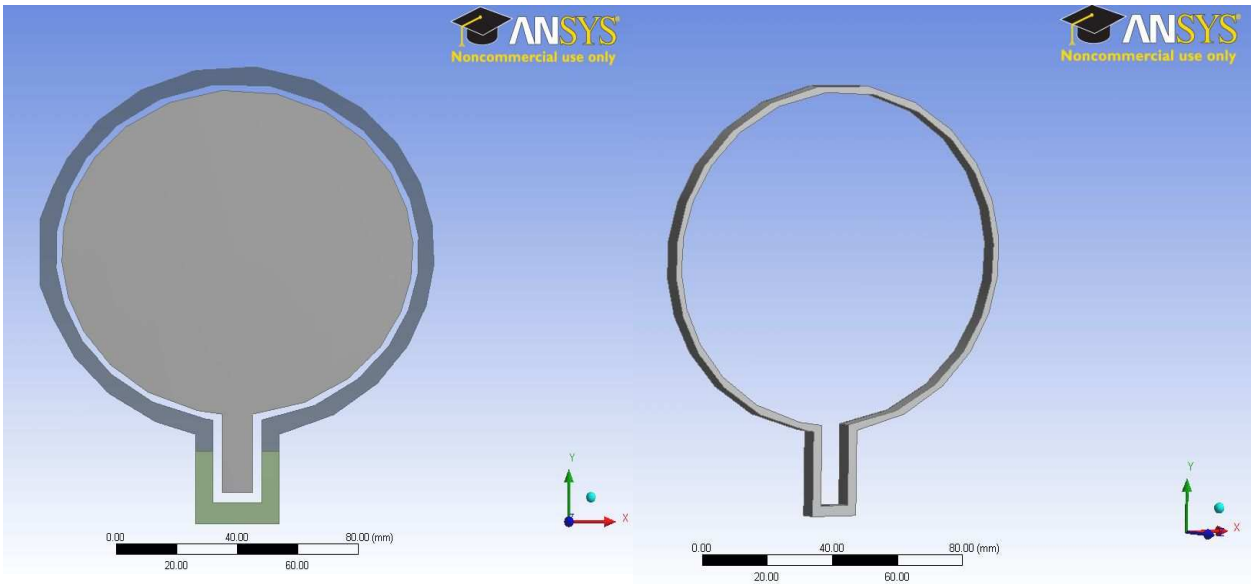

Figure 3.1 In the left picture the solid bodies are shown (Skull and Brain), CSF body is shown in the right picture

3.2 Mesh strategy

In order to achieve a proper mesh the body has been separated into three different parts (Skull, Brain and CSF) and the mesh is different for each part.

For the solid part two different meshing controls are used. Mapped face meshing control and edge sizing.
Mapped Meshing controls places a mapped face mesh control on quadrilateral and triangular faces for surface body models and only triangular faces for solid models. The application will automatically determine a suitable number of divisions for the edges on the boundary face. If the number of divisions is specified on the edge with a Sizing control, the application will attempt to enforce those divisions.

Edge sizing Control places the number of divisions in the marked edges. The application demands the number of divisions that the edge has to be split. This application results in a uniform mesh surrounding the edges.

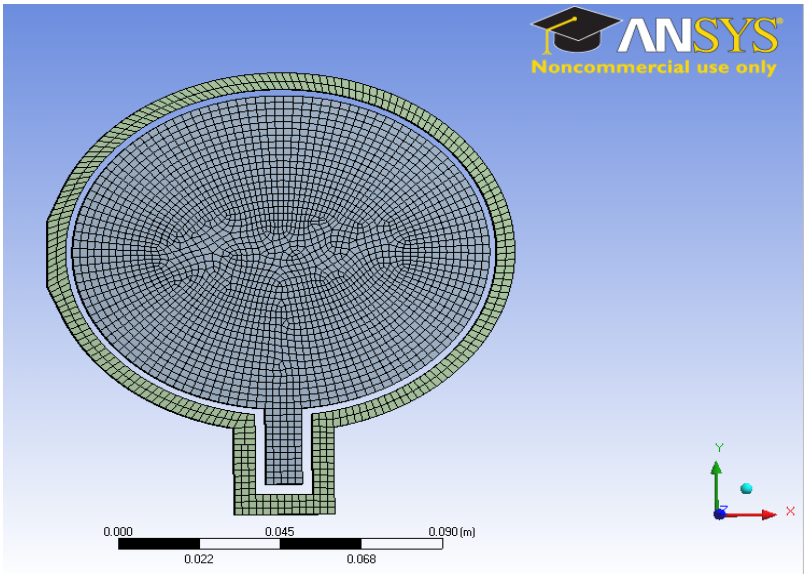

Figure 3.2 Mesh of the solid part

The CSF body is meshed in CFX-Mesh. The spacing between nodes has been controlled and the inflation has been added in order to reduce the number of nodes in the Z direction.

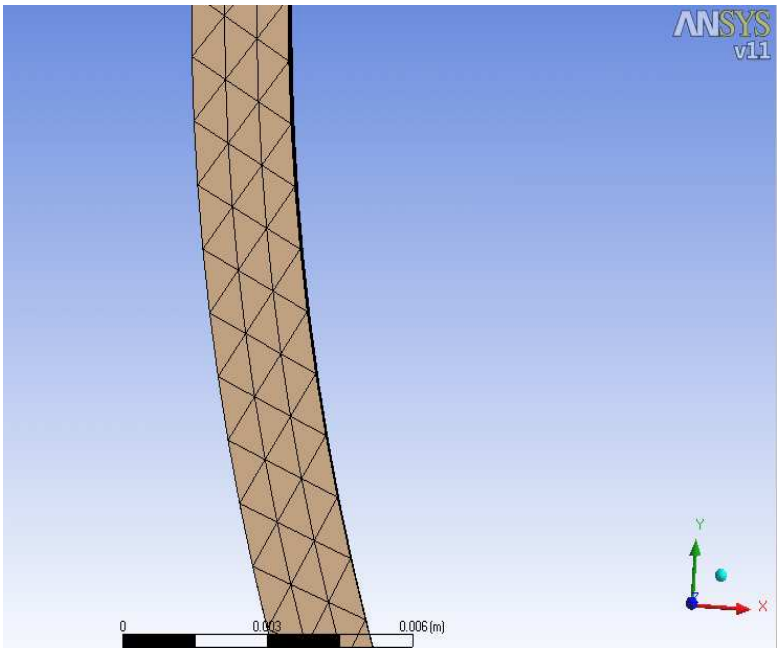

Figure 3.3 Mesh of the liquid part

3.3 Scenario

The next step is to prepare the test scenario. For this task the software used is simulation for the FEM part and CFX for the liquid part. It is important to remember that there are two different software programs working which have to be coupled.

Load applied

The idea is to simulate the impact of the head in a road traffic accident. In order to do so a force is applied to the front of the head as can be seen in the following picture:

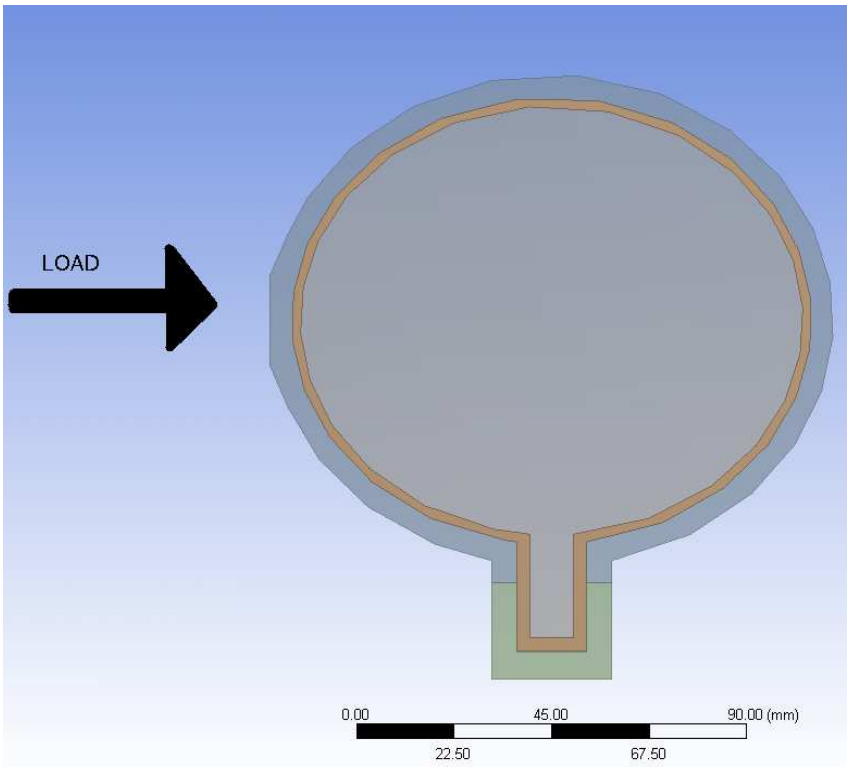

Figure 3.4 Sketch of the load applied

This part has been one of most challenging, after several attempts no solution could be found, so a change in the strategy had to be made. The next strategy was to apply acceleration but the same problems were found, the coupling was not able to run with such boundary condition.

The impossibility of neither applying a force nor an acceleration using Ansys has forced the use of another strategy. This strategy has been the application of a displacement depending on the time, acceleration of the head is forced as a result. The causes of why it is not possible

to apply any force still remains unknown.

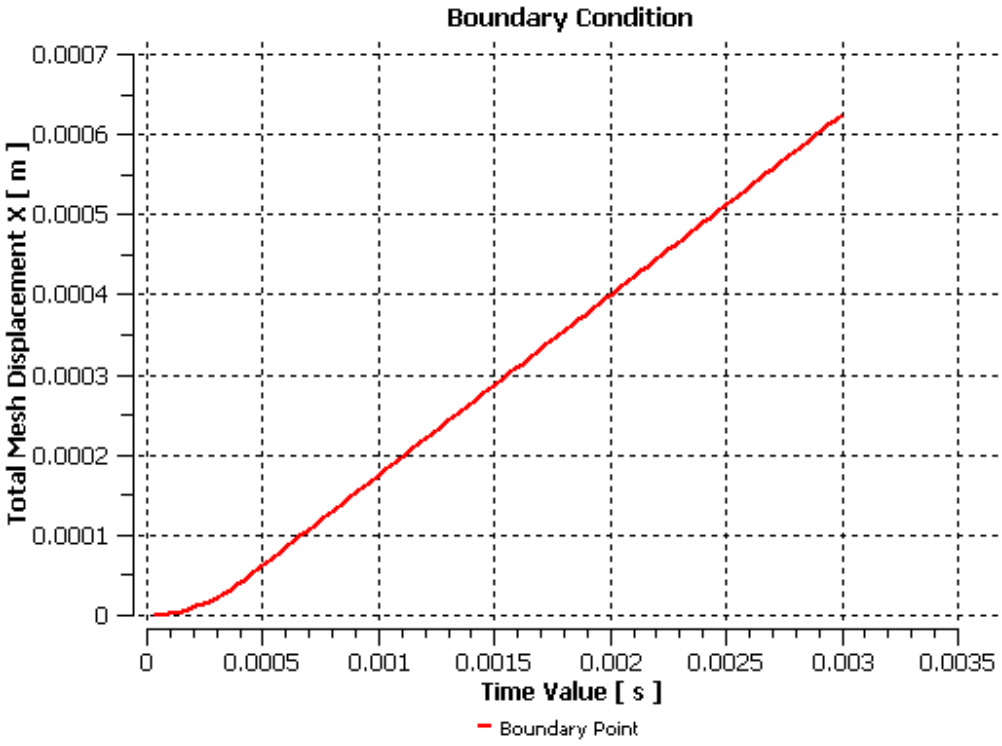

Figure 3.5 Displacement versus time

The displacement is applied during 3ms of the simulation; during the first 0,5ms a quadratic function is applied:

$$x(t) = \frac{1}{2}a_0 t^2 + v_0 t + x_0$$

Where a_0 = 500m/s^2; x_0=0m; v_0=0m/s.

After 0.5ms the displacement follows a linear function that implies zero acceleration and constant velocity.
The displacement is applied in the front part of the skull this part has been prepared flat in order to get a displacement along the x axis.

One of the most interesting points is to know how the wave propagation influences in the brain injury. So the suitable time simulation has to be tested in order to let the wave propagation flow all over the whole head. The time of 3 ms is enough to study the effect of the wave propagation.

3.4 FEM Configuration

Once the mesh has been created the simulation type has to be set. The simulation type for a

time dependent deformation is "Flexible Dynamic", this simulation type also allows the coupling between CFD and FEM software.

Boundary conditions

There are several boundary conditions in the solid bodies, these are:

- symmetry in the lateral faces in order to achieve the 2D model
- frictionless support at the bottom of the neck
- fluid- solid interfaces, this boundary condition is especially important due to the fact that it is the one that connects the two software programs (Ansys and CFX)
- displacement in the X direction (mentioned above)

Solid Material Properties

As has been mentioned before the skull is elastic material and the brain is hyper-elastic. The following table contains the properties of each material

Properties	**Brain**	**Skull**	**Neck**
Density(Kg/m^3)	1040	1420	1420
Thermal expansion (1/ºC)	0.1	0.1	0.1
Young´s Modulus (Pa)	None	6.5E+009	6.5E+006
Poisson´s Ratio	None	0.22	0.22
Ogden Parameters			
Material Constant μ_1(Pa)	290.82	None	None
Material Constant a_1	6.19	None	None
Incompressibility Parameter d_1	2.09E-007	None	None

These are standard properties for the materials. The influence of the densities is also compared in the final result. Thus the density of the brain is changed to higher and lower values (900 and 1100 Kg/m3). It is believed that the density ratio between the CSF and the brain has an important influence on the coup-contre-coup. However, in this thesis the factor that has been modified is the Young´s modulus of the skull. In order to study its influence, a very stiff skull ($E= 6{,}5*10^{12}$) and a very soft skull ($E=6.5*10^{6}$) are tested and compared.

Once the setup is finished the Ansys input file is created, this file contains all the information about the Solid part. The file is charged in the CFX in order to share the information and establish the coupling between them.

3.5 CFD Configuration

The CFX configuration type is transient and the coupled solver is executed. The fluid is setup to be compressible, so the Total energy equation is required; this option is demanded by the software even though the heat transfer is not taken into account in the final analysis. The fluid is laminar due to the flow being very low, at least in principle.

Boundary conditions

- symmetry in the lateral faces in order to achieve the 2D model
- fluid- solid interfaces (Skull-CSF, CSF- Brain)

Liquid material properties

The CSF has been modeled as water, because its properties are very water-like and there is not an exact value for the density. It is believed that there is a relation between the brain-CSF density ratio and the coup contre-coup effect. This is another aspect to be studied. The liquid is lightly compressible; this factor can be modeled as compressible if the density is dependent on the pressure. Thus CSF has the same properties as water.

3.6 Analysis settings

Analysis settings have to be configured both in FEM software and CFD software. According to FEM Simulation the Step end Time (Total time) is 3ms and the time step is 0.03ms. This time step has been learned from experience during testing and after some simulation this time step gives enough stability to converge. This time step also gains accuracy and the possibility of studying the wave propagation, because taking into account the speed of sound in water (1500m/s) it takes almost 0.1 ms to pass through the whole body.
According to the CFD analysis settings both the total time and the time step have been configured with the same values as the FEM settings, in order to get more stability in the coupling. In a coupled solution the CFD and FEM solver are running parallel and exchanging their results. The load and the force are transferred through the boundary conditions "solid-liquid interface". Another factor that is controlled is the under-relaxation factor, this one allows more stability to be obtained. After several simulations it is possible to analyze the oscillations. This factor reduces these oscillations between the two solvers. After several attempts the under-relaxation factor is set to 0,9.

4 RESULTS

The results that have been obtained are calculated in different cloud points from the skull, the brain and the CSF. In addition, contour plots and videos have been designed to give a general overview of the interaction between the three parts in each time step.
To know the magnitude of the deformation, the total equivalent strain and the total mesh displacement have been extracted from the brain. Regarding the liquid, the total pressure has been the most relevant result and usually has helped to understand the behavior of the equivalent strain and the brain mesh displacement. For the skull, the mesh displacement has been checked to see the influences of the boundary conditions. Additional results have been extracted from the simulations, they can be found in the appendix.

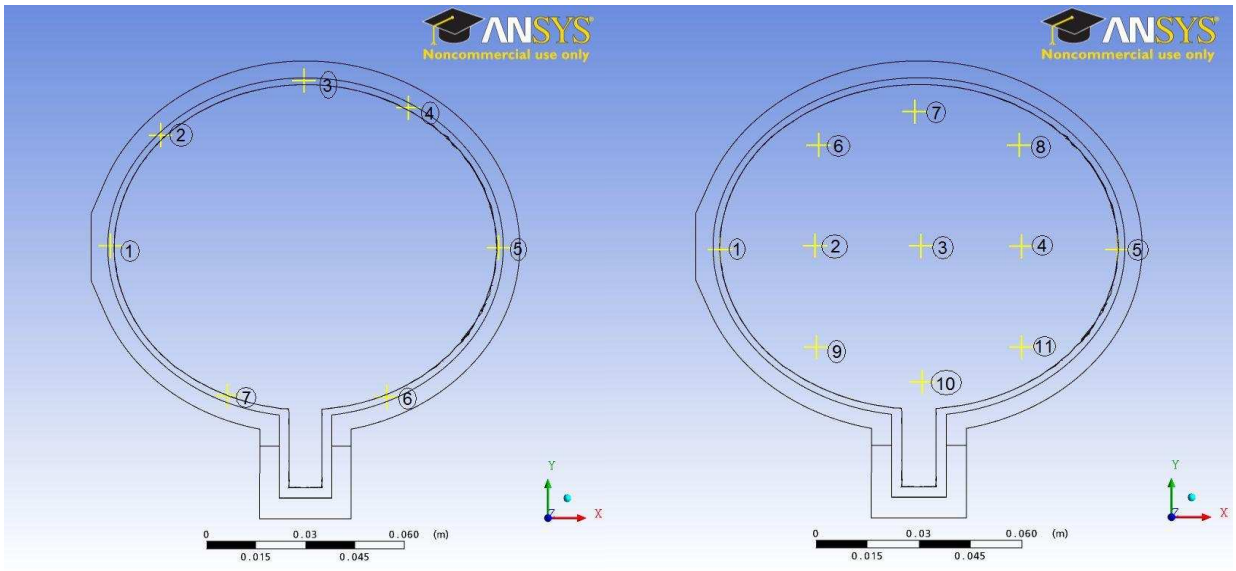

Figure 4.1. & Figure 4.2. Cloud points from CSF and brain respectively

The studied points in the liquid have been located around the CSF. The same for the brain, but the most interesting point is the number 5, where the contrecoup effect is expected. The others have helped to understand the mechanical behavior and how the wave propagation affects the brain. In the skull, 4 points have been marked to know the relative displacement between the front and the back.

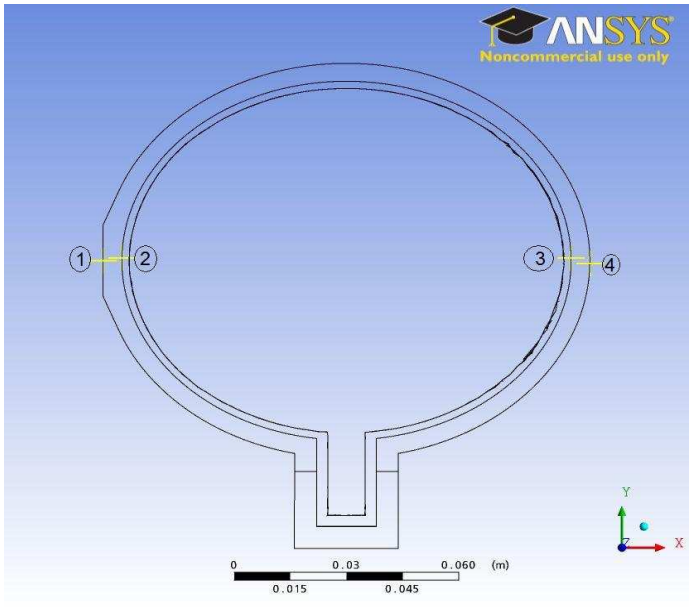

Figure 4.3 Cloud points located in front and the rear of the skull

Two simulations are shown. The first one with the material data that has been mentioned before, see section 3.4, and in the second simulation the skull and neck stiffness has been increased by a factor of 1000. That mirrors an unrealistic scenario but it is useful to know the influences of the skull and neck stiffness in the results. The boundaries and the other parameters remain the same as described above.

In both simulations the velocity of the fluid has been checked in order to verify that the Reynolds number in the channel where CSF is located always remains under Re < 2300 (hypothesis of laminar flow).

$$Re=\rho VD/\mu \qquad \text{Eq 4.1}$$

4.1 Simulation 1

First of all, the pressure has been studied in all the 7 points of the CSF. Looking at the graphs one can see that the pressure peaks correspond with the points placed close to the front and to the back respectively, where the contrecoup may occur. It is also noticeable that, at the beginning, the pressure tends to be positive close to the boundary where the displacement is applied and negative at the back. In addition, after 0.5 ms that is, when the acceleration is zero, the pressure in L1 (close to the front) starts to decrease which is reasonable.

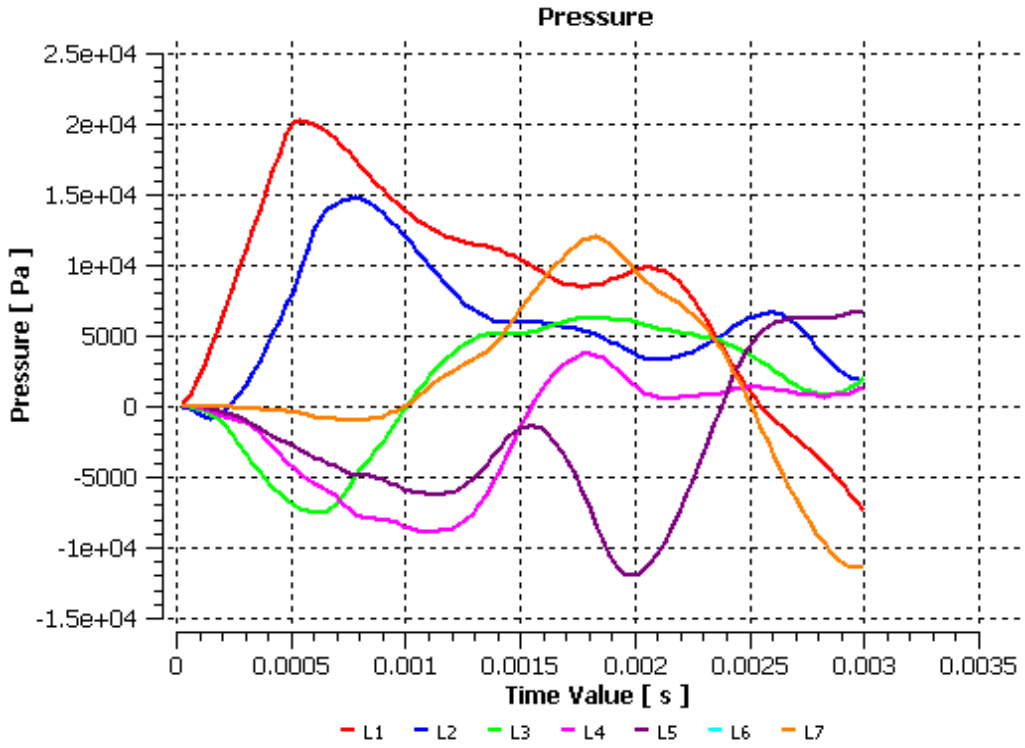

Figure 4.1.1 Pressure plot of points 1 to 7 placed within the fluid (CSF)

To check out the time that the pressure wave takes to go from the front to the back part (from point 1 to 5) a simulation of just 0.2 ms has been run (with a time step of 0.01 ms). According to Section 3.6, the calculated time is 0.1 ms which corresponds to the delay of point 5. Looking at the following graph the period of time between when the pressure L1 starts to increase and the pressure L5 feels the effect of the load displacement is approximately 0.1 ms.

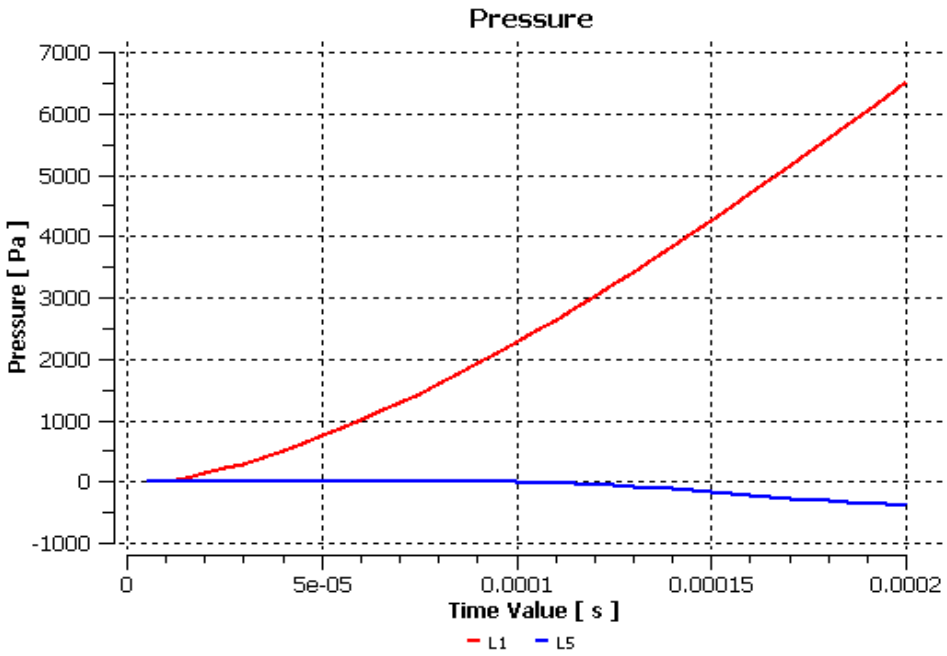

Figure 4.1.2 Pressure plot of points 1 and 5 within the fluid

The displacement of the mesh has been calculated in all the points mentioned before. The most relevant points are the ones placed inside the brain, which try to follow the boundary condition. B1, B2 and B3 are located closer to the front part, hence they imitate the displacement of the boundary with a delay. On the other hand, B4 and B5 show a certain disorder and nonlinearity.

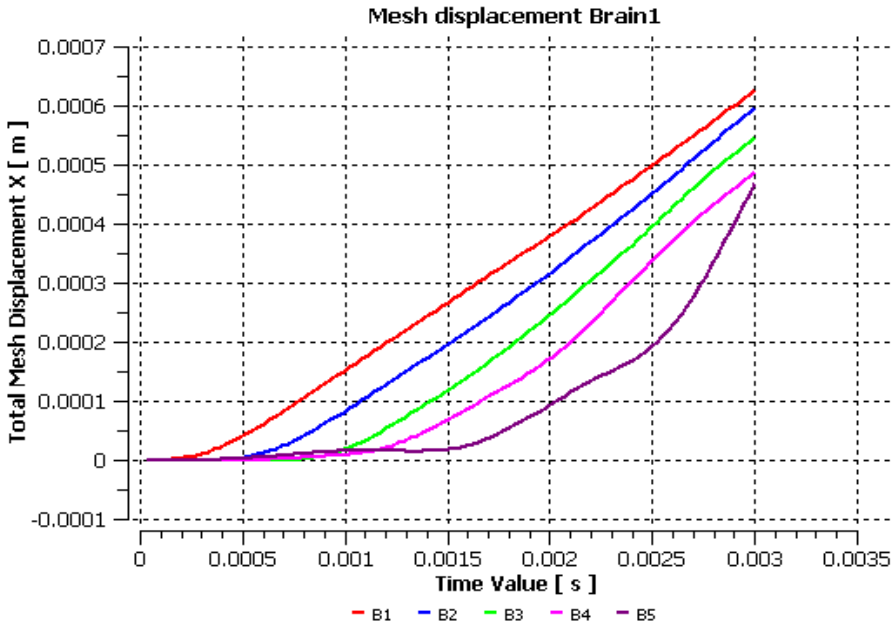

Figure 4.1.3 Mesh displacement of points 1 to 5 placed in the brain

To understand the effects of the boundary applied the relative displacement between different nodes has been calculated. Firstly the nodes inside the brain and in X direction are studied. Looking at the graph 4 shown below, a compression in X direction can be observed because all the pairs of points have a negative displacement. The most significant relative translational is the pair B5/B1, which are the ones located in the back and frontal part of the brain respectively.

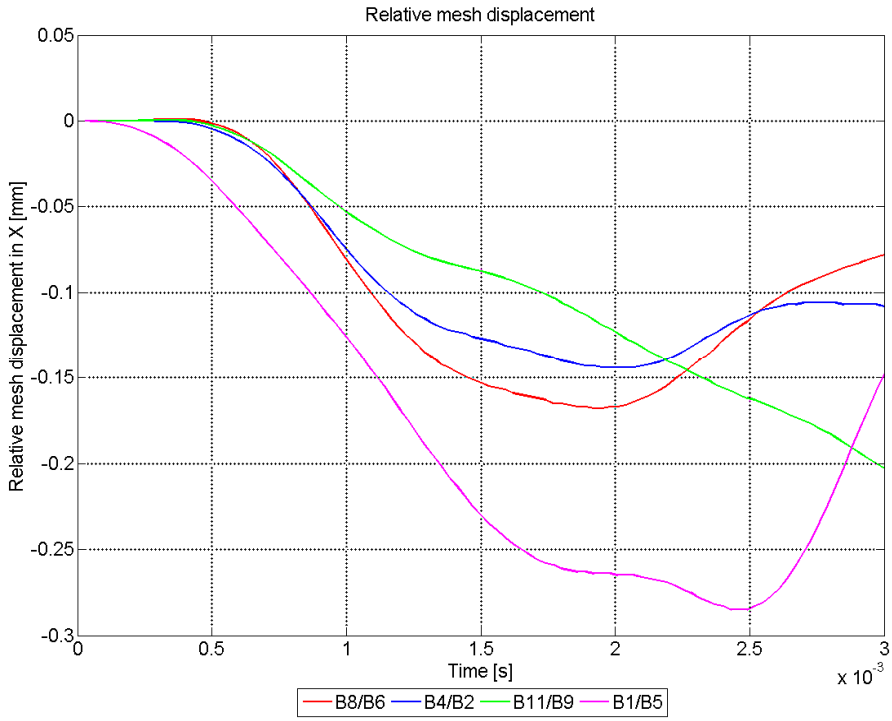

Figure 4.1.4 Relative mesh displacement in X direction of points 8/6, 4/2, 11/9 and 5/1 placed in the brain

Taking a look to the points located in the skull, the relative displacement between them also shows that a compression is affecting the model.

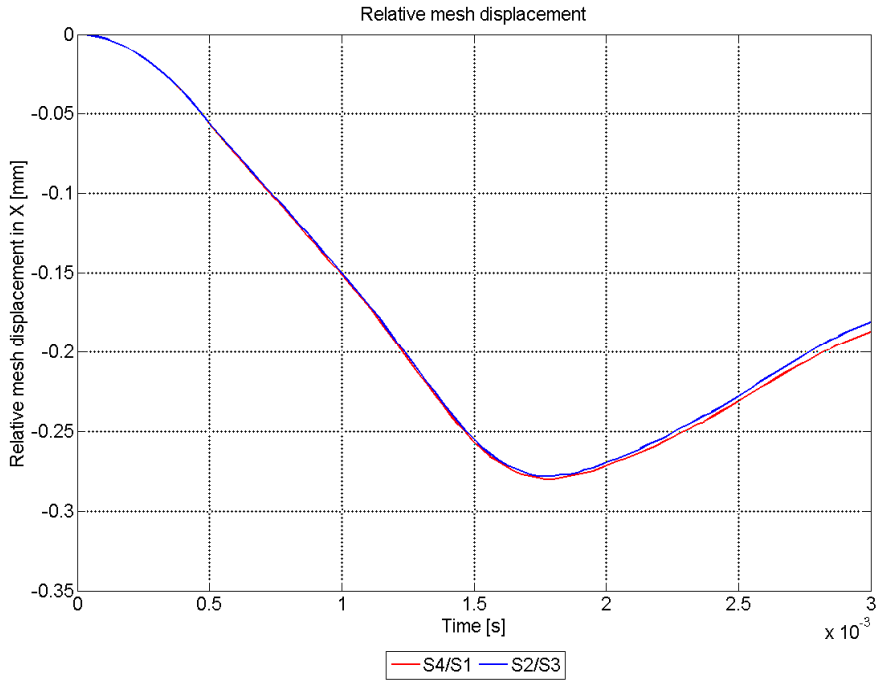

Figure. 4.1.5 Relative mesh displacement in X direction of points 4/1 and 2/3 placed in the skull

On the other hand, when the relative mesh displacement is plotted in Y direction the expansion is present in all the pairs of points.

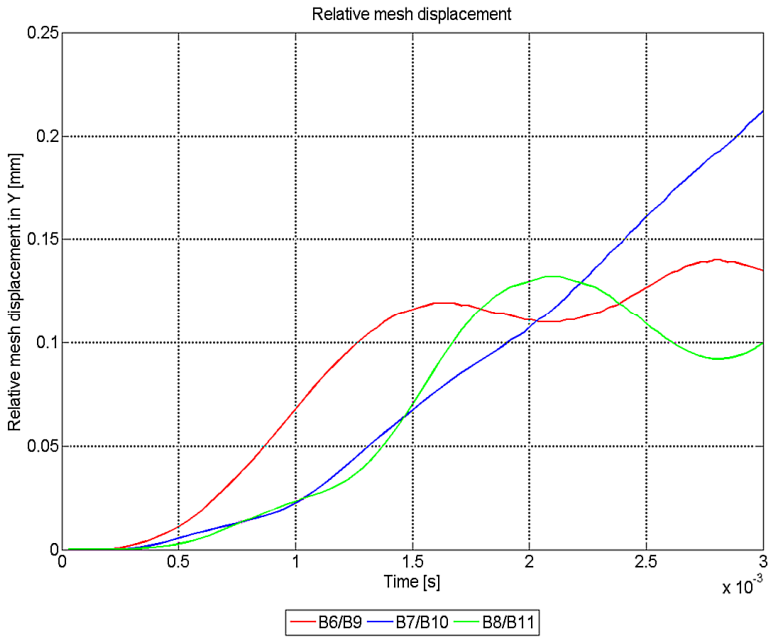

Figure 4.1.6 Relative mesh displacement in Y direction of points 6/9, 7/10 and 8/11 placed within the brain

The next graph shows the relative mesh displacement between points located in the skull and brain. The aim of this graph is to check whether there is contact between them at any moment in the experiment

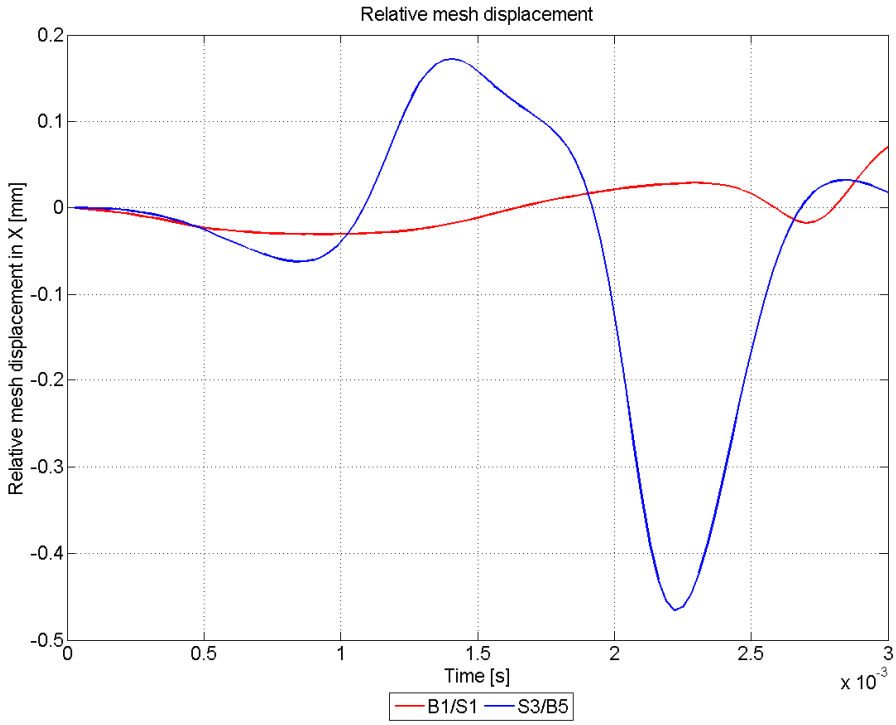

Figure 4.1.7 Relative mesh displacement in x direction between brain and skull

It can be seen that the maximum compression of the liquid part is less than 0.5mm, this is occurring in the back part of the head between the brain point 5 (B5) and skull point 3 (S3), that means that contact between skull and brain does not occur because the thickness of the CSF is 2mm.

To estimate the deformation of the brain, as it has been mentioned in section 1.3.2, the strain is a good indicator of the tissue damage and thus, the brain injury level. Hence, the Total Equivalent Strain has been calculated in the points placed within the brain.

The most crucial zone is where point 5 is located. It shows a peak of more than 6% of deformation at 2.5 ms, which corresponds when the relative mesh displacement between point 5 and 1 has the highest value and, thus, the maximum compression, see fig. 4.1.4

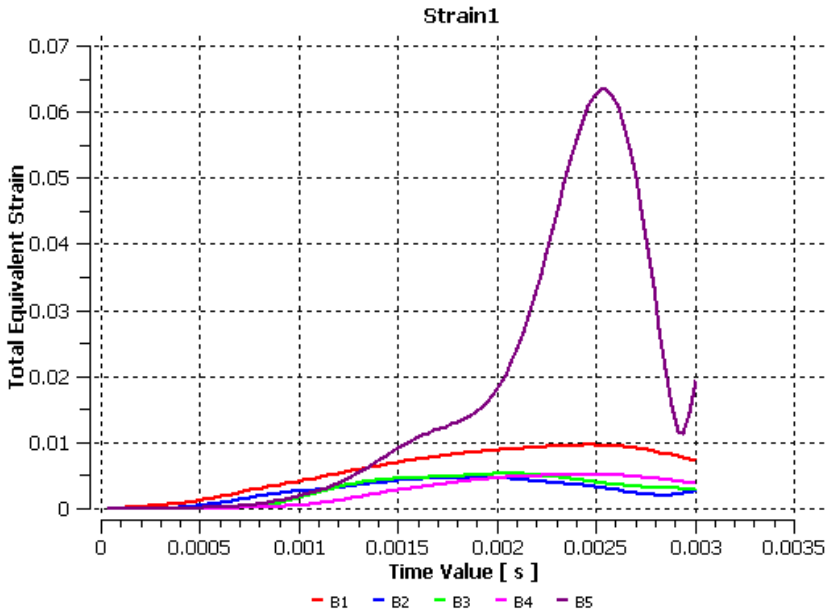

Figure 4.1.8 Total equivalent strain of points 1 to 5 placed within the brain

4.2 Simulation 2

Another model has been created with different skull stiffness, the Young´s modulus has been increased 1000 times. The other parameters remain exactly the same. In this part a comparison between this new skull and the original one is made.
The following graph relates to the pressure inside the liquid:

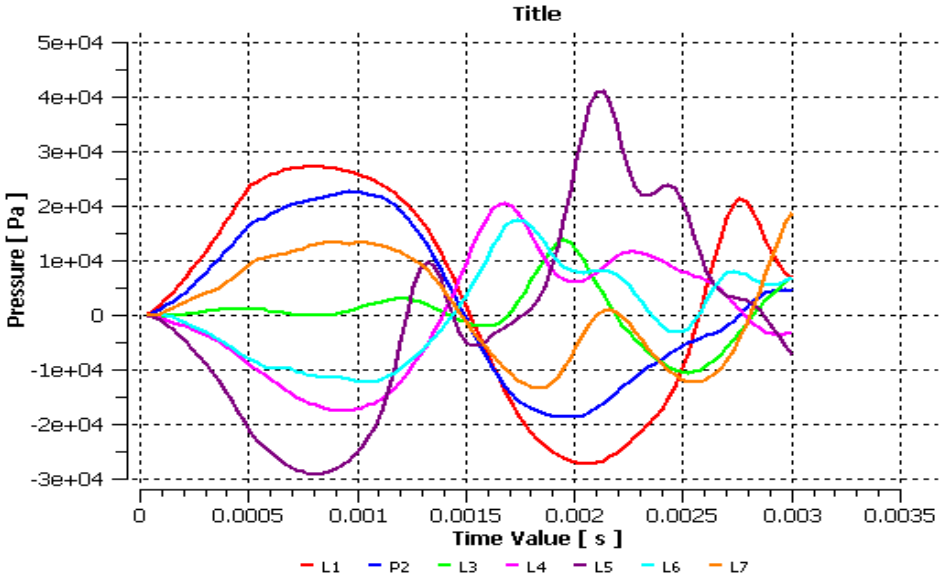

Figure 4.2.1 Pressure inside the CSF

The pressure inside the CSF is higher than the pressure in the original skull. The point number 5 suffers the maximum pressure, at 0,8ms the pressure in this point is -2.85 Pa, while at 2.15ms the pressure is 4.15 Pa. the other most significant is the number 1, this one which is placed in the front part of the head has higher values than the original value.
There is a phenomenon that takes place before 1.5ms; this phenomenon is that all the pressure waves change their signs, and if the relative mesh displacement of the skull is analyzed it can be seen that this phenomenon happens when the compression of the skull becomes expansion

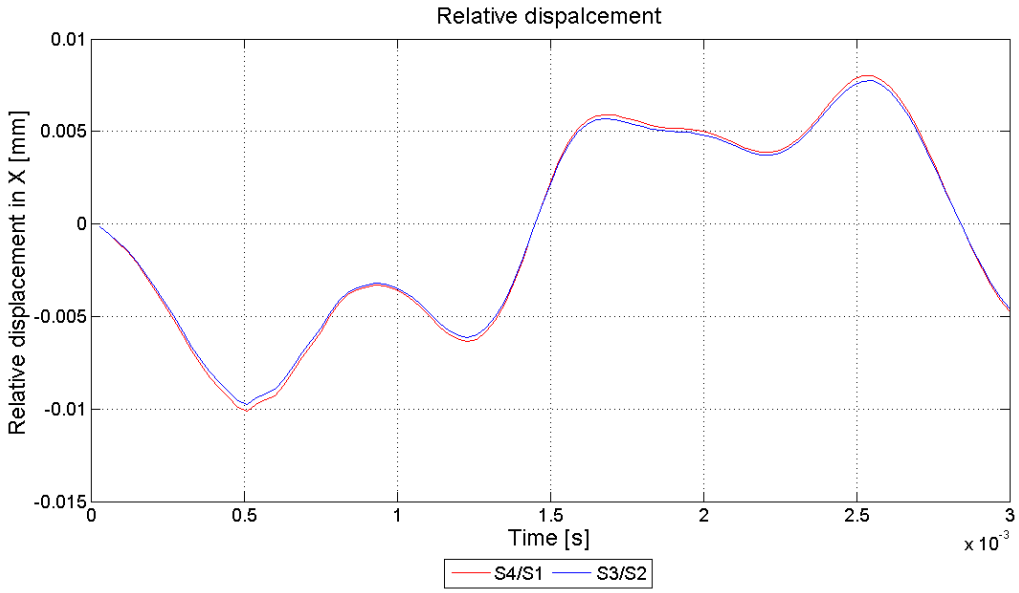

Figure 4.2.2 Relative displacement in x direction inside the skull

In this figure it is shown how the skull is compressed and then is expanded, this is occurring in the x direction (see points of the skull in fig 4.3). Comparing that plot with the original one it can be seen that the compression rate is lower because this skull is very rigid. More compressions and expansions can be observed in the same period of time because the sound propagation is depending on the Young´s modulus. The next graph is related to the total mesh displacement inside the brain in x direction:

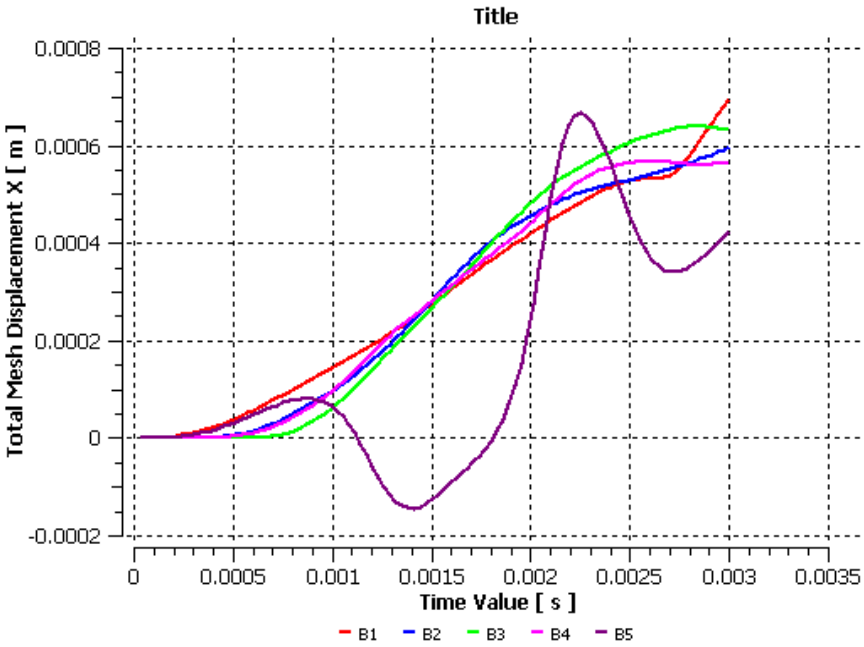

Figure 4.2.3 Total mesh displacement in x direction inside the brain

All the points inside the brain are trying to follow the boundary condition except the point number 5 (see fig 4.1). This point even moves in the opposite direction causing a significant mesh displacement (see Fig 4.2.4) and Total Equivalent Strain (see Fig 4.2.5). The rest of the points are in their original position at 1.5 ms. The change in the sign of the pressure waves and of the compression of the skull to expansion is also happening at this moment.

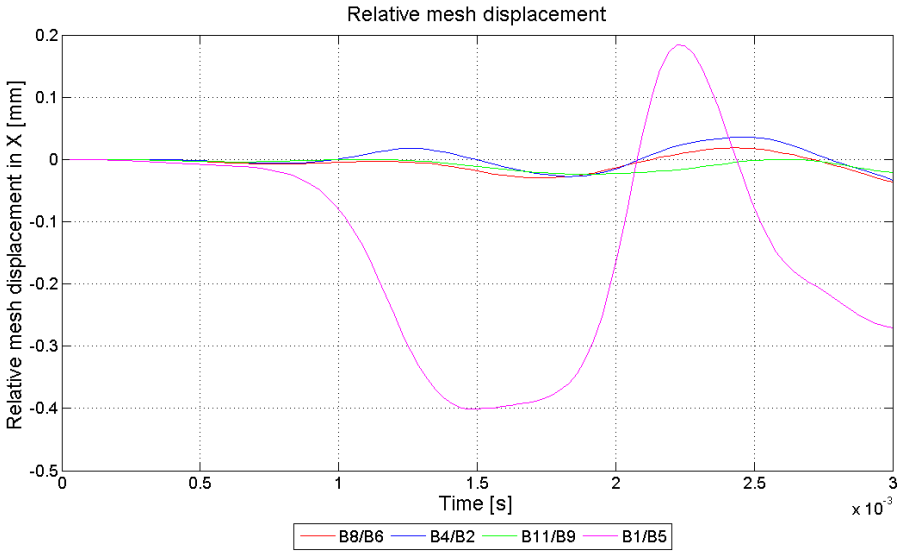

Figure 4.2.4 Relative mesh displacement inside the brain

Regarding the total equivalent strain inside the brain:

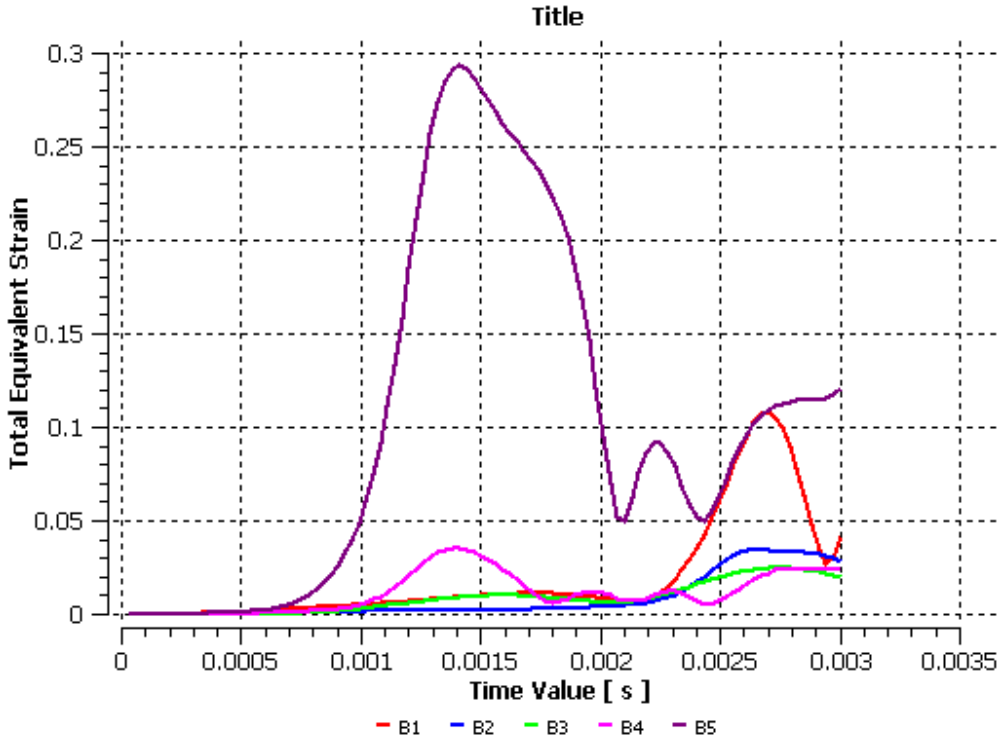

Figure 4.2.5 Total equivalent Strain inside the brain

The total equivalent strain is significantly higher than in the original experiment, about five times higher. The maximum peak occurs before it did in the original experiment.In the new skull the peak appears at 1.4ms.
This maximum peak also occurs when the pressures waves inside the CSF are changing their sign.

Conclusions

Numerical simulation of traffic-related brain injuries has been a challenge due to the fluid solid interaction within the brain. That has meant that the main part of the thesis has been to build a model which may be able to work. One of the scopes was to apply either a force or acceleration in order to control the load. Due to the complexity of the scenario it has not been possible to achieve this task. On the other hand acceleration was applied indirectly by using a linear displacement depending on time.

Parts of the results have been predictable such as the compression in the X direction or the expansion in the Y direction. However the main effect that was expected (coup) does not appear in the simulation, however the countre-coup is found.

It has not been possible to find a relation between the pressure inside the CSF and the strain in the Brain. Nevertheless in the second simulation (with the rigid skull) some relation between the pressures inside the CSF and the mesh deformation in the brain and skull appears.

The duration of the simulation has been 3ms, so the steady state of the bodies has not been reached. The perfect duration would be the one which is able to reach that state.

One has to be very skeptical when the results are analyzed. There is still a lot of research to do in this area. The boundary conditions have to be changed, the head has to have freedom of movement in all directions. Secondly a 3D model is needed in order to validate the results with real experiments and a more complex geometry is required. For example, the thickness of the skull and the CSF are not uniform; but one of the biggest problems that one has to deal with is the capability of the CSF to control the brain pressure, this effect can make a big difference in the results.

After all those problems and the impossibility of validation with real experiments it can be shown how the interaction between the solid and the liquid takes place within the head. Simulations are very important in vehicle safety, which is why more investigations are needed in order to predict and to understand the injury mechanism in accidents.

References

[1] Ansys Release 11.0 Engineering Data Help, 2007

[2] Z.Brinkerhoff. *Reflexology.* Modern Institute of Reflexology. <www.reflexologyinstitute.com>

[3] Britannica Encyclopaedia. *Anatomy: Pia Mater.* <http://www.britannica.com>

[4] Center For Brain Injury and Repair, University of Pennsylvania. *Traumatic brain injury: a "silent epidemic".* <http://www.neuroskills.com/epidemiology.shtml>

[5] Center Neuro Skills. *Epidemiology of TBI.* 1 May 2008 <http://www.neuroskills.com/epidemiology.shtml>

[6] J. Davidsson. *Passive Safety Lecture Notes.* Chalmers University of Technology

[7] DUI Attorney Directory. *Alcohol Information.* <http://www.duiattorneydirectory.com>

[8] E. Finkelstein, P. Corso, T. Miller. *Incidence and Economic Burden of Injuries in the United States.* Oxford University Press, USA, 2006

[9] J. Fliedner. *Development of a Brain Model for Simulations of Diverse Types of Injuries.* Departmant of Applied Mechanics. Chalmers University of Technology. Göteborg Sweden, 2008

[10] G. Franceschini (2006). *The Mechanics of Human Brain Tissue.* Modeling, Preservation and Control of Materials and Structures, University Of Trento.

[11] C.W. Gadd. *Criteria for injury potential. Impact Acceleration Stress Symposium.* National Research Council publication no 977. National Academy of Sciences, Washington DC pp141-144, 1961

[12] Greenberg & Rudman LLP. *Concussion from an accident.* Los Angeles Injury Lawyer Blog <www.los-injury-lawyer-blog.com>

[13] Hindawi. *Cortical Contusion.* <www.hindawi.com>

[14] M. L. Itkis, G. I. Mchedlishvili. *Method of Determining the Mechanical Properties of the Brain in Vivo.*

[15] J. Ivarsson. *Physical Modeling of Brain and Head Kinematics.* Department of Machine and Vehicle Systems. Chalmers University of Technology. Göteborg, Sweden, 2002

[16] S. Kleiven, (2002). *Finite Element Modeling of the Human Head.* PhD thesis, Department of Aeronautics, Royal Institute of Technology, Stockholm, Sweden.

[17] J.A. Langlois, W. Rutland-Brown, K.W. Thomas. *Traumatic Brain Injuries in United States.* Division of Injury Response National Center for Injury Prevention and Control Centers for Disease Control and Prevention U.S. Department of Health and Human Services <www.cdc.gov/injury>

[18J. Lubliner (2008). *Plasticity Theory (Revised Edition)*. Dover Publications. ISBN 0486462900. http://www.ce.berkeley.edu/~coby/plas/pdf/book.pdf.

[19]G. Mase,. (1970). *Continuum Mechanics*. McGraw-Hill Professional. ISBN 0070406634.

[20] E.M. Marieb, (1998), *Human Anatomy an Physiology.* Fourth edition. Addison-Wesley

[21] J. H McElhaney, J. L Fogle, J W. Melvin, R. R. Haynes, V. L. Roberts, and N. M Alem. *Mechanical properties of cranial bone.* J. Biomech. , vol3, pp. 495-511, 1970

[22] G.B. McHenry. *Head Injury Criterion and the ATB.* McHenry Software, Inc.

[23] D. F. Meaney, A. C. Bain. *Tissue Level Threshold for Axonal Damage in an Experimental Model of Central Nervous System White Matter Injury.* Journal of Biomechanics, 33:1369-1376, 2000.

[24] Medical Look. *Brain ventricles and CSF.* <www.medical-look.com>

[25] Merck & Co., Inc. *Intracranial Hematomas.* <www.merck.com>

[26] F. Su. *Modeling of Brain Tissue as Porous Visco-Hyperelastic Medium.* Master's thesis, Department of Applied Mechanics, Chalmers University of Technology. Göteborg, Sweden, 2007

[27] M. Mokabberian. *Choice of Proper Model for the Solid Skeleton of Brain Tissue Based on Consolidation Tests.* Department of Applied Mechanics, Chalmers University of Technology. Göteborg, Sweden, 2007

[28] N. Nakamura, H. Masuzawa, H. Sekino, H. Kono, A. Kikuchi, K. Ono. *Which is the More Severe Impact on the Head: Sagittal or Lateral?* Head and Neck Injury Criteria. National Highway Traffic Safety Administration. U.S. Department of Transportation.

[29]D. Rees (2006), *Basic Engineering Plasticity - An Introduction with Engineering and Manufacturing Applications*, Butterworth-Heinemann, ISBN 0750680253

[30] D. H. Robbins, J. L. Wood. *Determination of Mechanical Properties of the Bones of the Skull*. 1969

[31] A.W. Selassie, M.L. McCarthy, P.L. Ferguson, J. Tian, J.A. Langlois. *Risk of posthospitalization mortality among persons with traumatic brain injury*. Department of Biostatistics, Bioinformatics, and Epidemiology, Medical University of South Carolina, Charleston, SC 29425, USA.

[32] M. Y. Svensson. *Neck-Injuries in Rear-End Car Collisons-Sites and Biomechanical Causes of the Injuries, Test Methods and Preventive Measures.* Doctor Thesis. Safety Division at Chalmers University of Technology. Göteborg, Sweden, 1993

[33] A. Thomas, M.D. Gennarelli. *Mechanistic Approach to the Head Injuries: Clinical and Experimental Studies of the Important Types of Injury.* Head and Neck Injury Criteria. National Highway Traffic Safety Administration. U.S. Department of Transportation

[34] D.J. Thurman, C. Alverson, K.A. Dunn, J. Guerrero, J.E. Sniezek. *Traumatic Brain Injury in the United States: A Public Health Perspective.* National Center for Injury Prevention and Control, Centers for Disease Control and Prevention, Atlanta, Georgia 30341-3724, USA.

[35] S. Timoshenko, J. N. Goodier. *Theory of Elasticity.* Second Edition. McGraw-Hill Book Company, Inc. 1951

[36] H. K. Versteeg, W. Malalasekera. *An Introduction to Computational Fluid Dynamics.* Second Edition. Pearson Prentice Hall. 2007.

[37] K. Weinberg: Lecture Notes for *Zur Methode der finiten Elemente in der Mechanik II: Nichtlineare Probleme*, TU Berlin

Appendices

Simulation 1

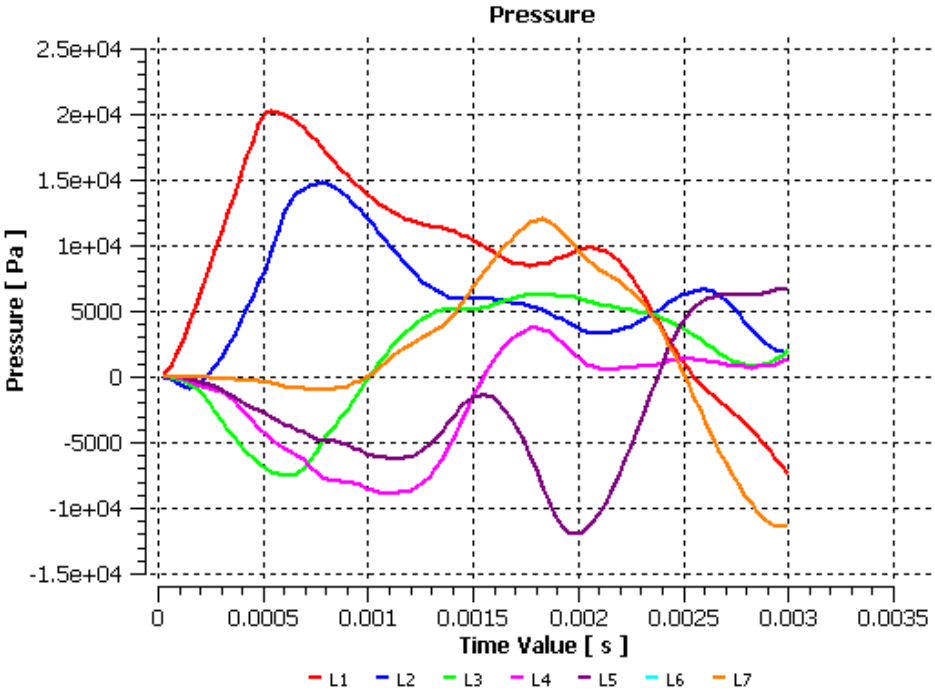

Figure A1 Pressure inside the CSF

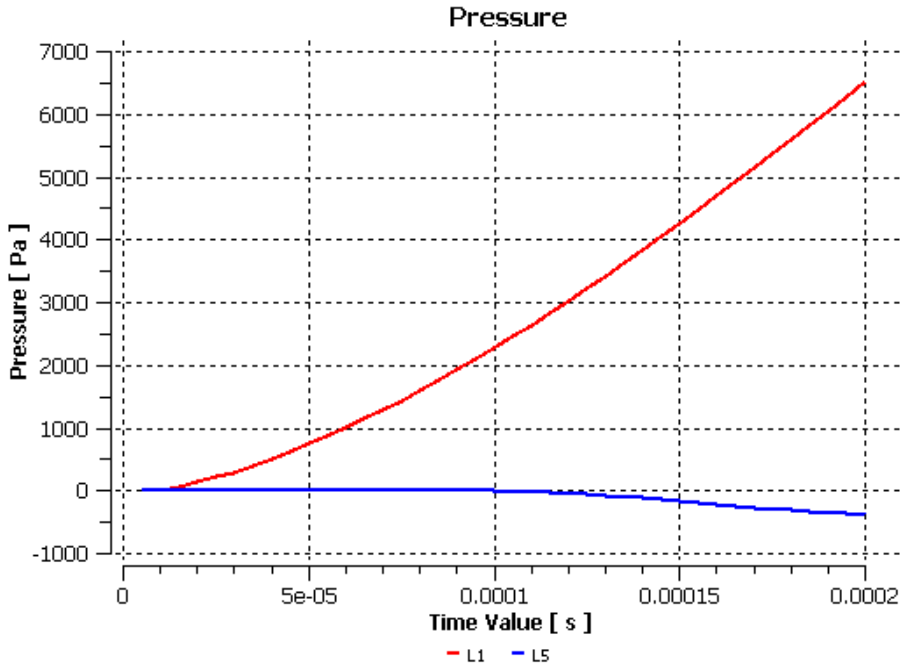

Figure A2 Pressure inside the CSF

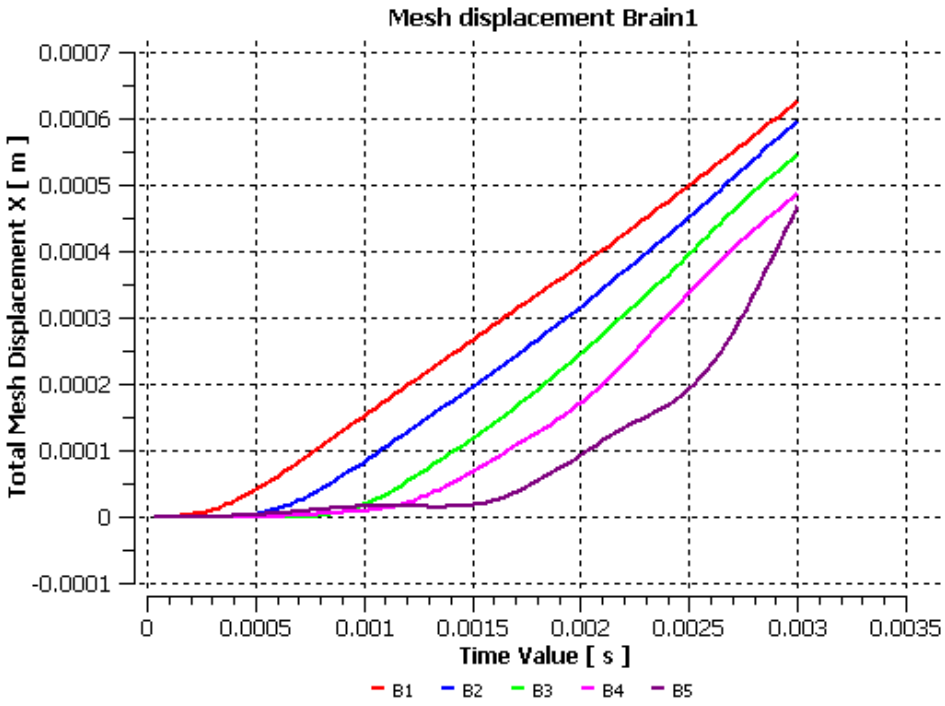

Figure A 3 Total mesh displacement inside the Brain

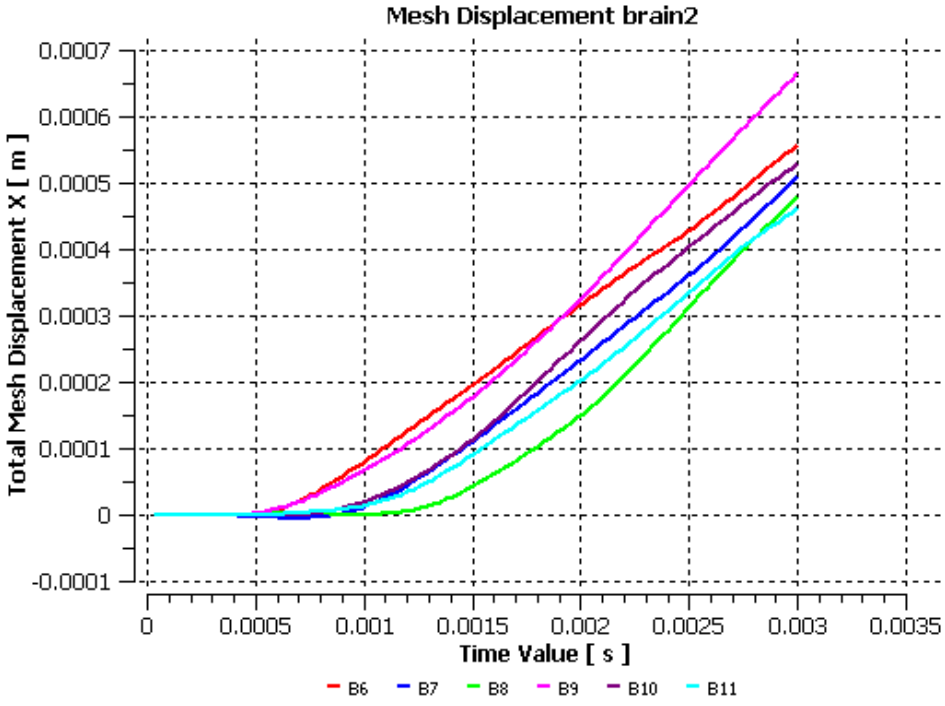

Figure A 4 Total mesh displacement inside the Brain

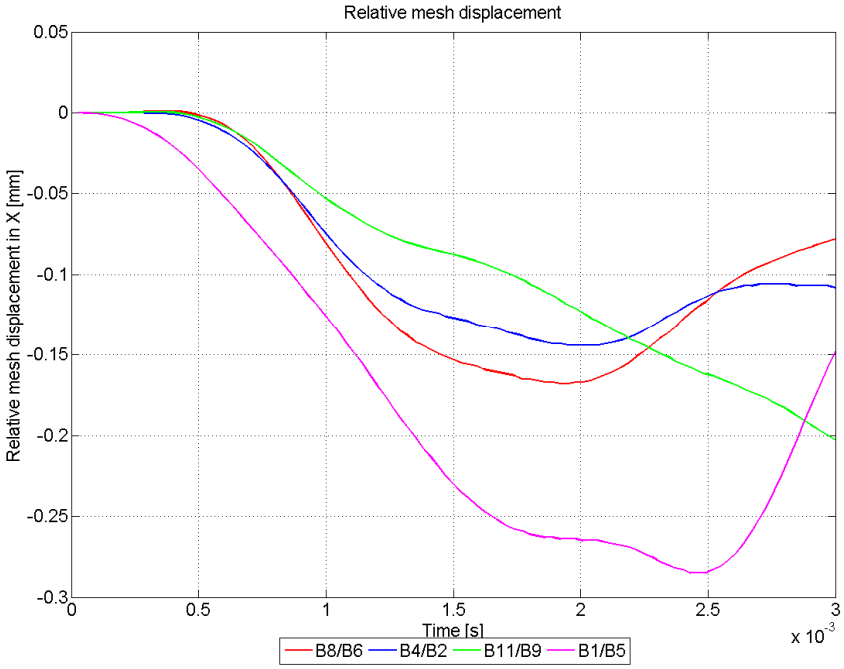

Figure A 5 Relative mesh displacement of brain points in x direction

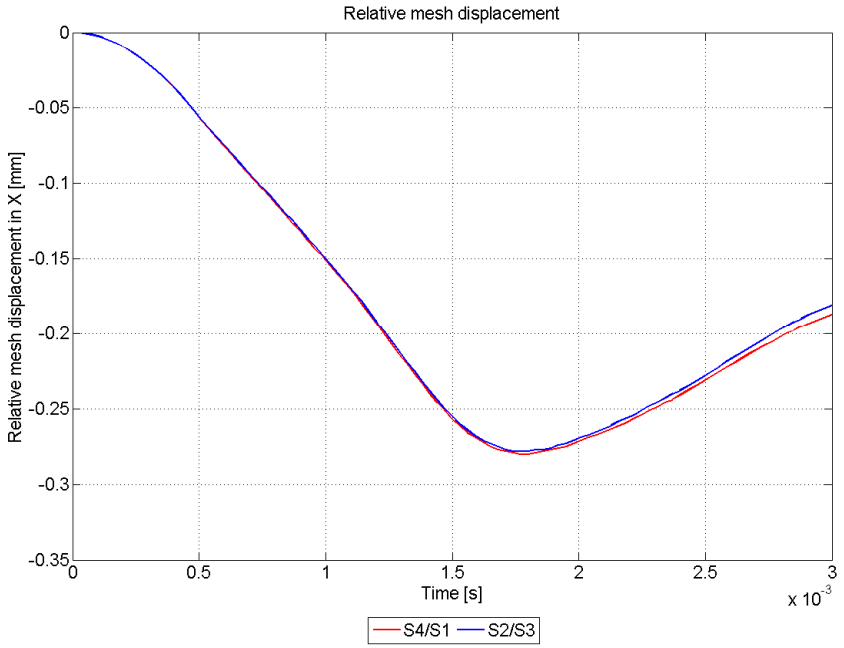

Figure A 6 Relative mesh displacement of skull in x direction

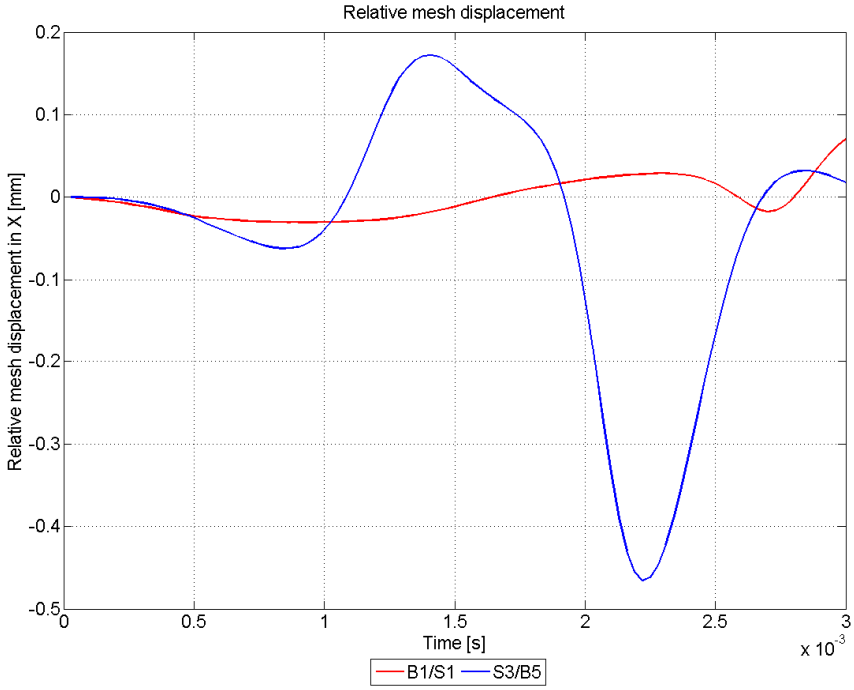

Figure A 7 Relative mesh displacement in X direction between brain and skull

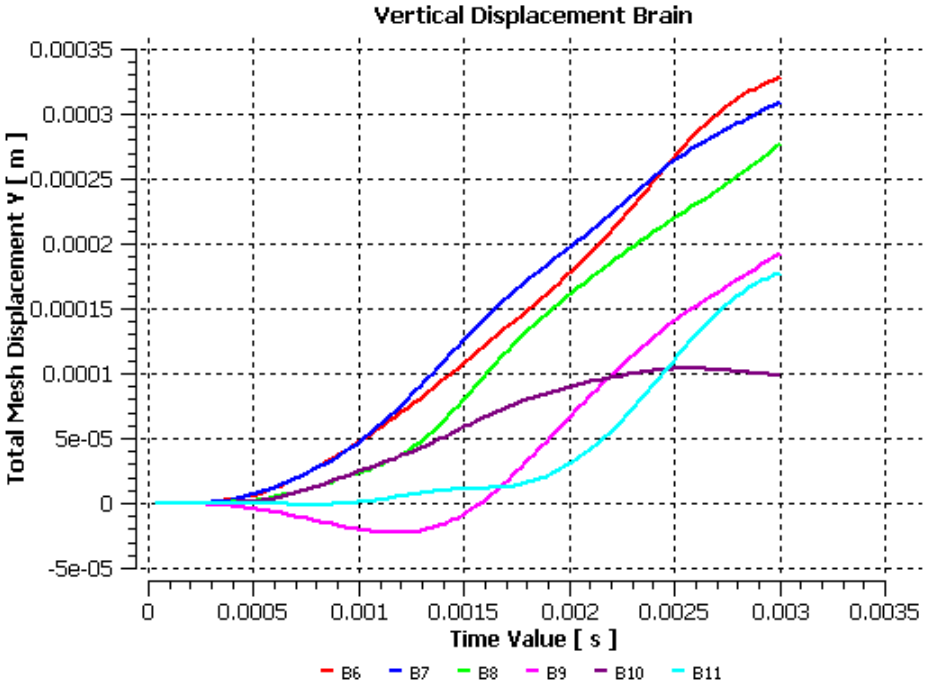

Figure A 8 Total mesh displacement in Y direction of the brain

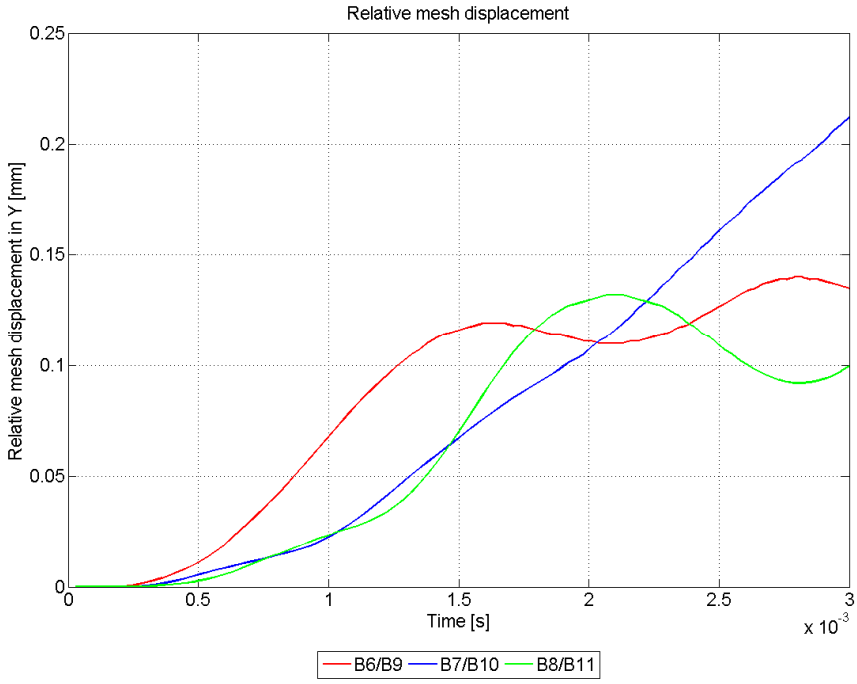

Figure A 9 Relative mesh displacement in Y direction of the Brain

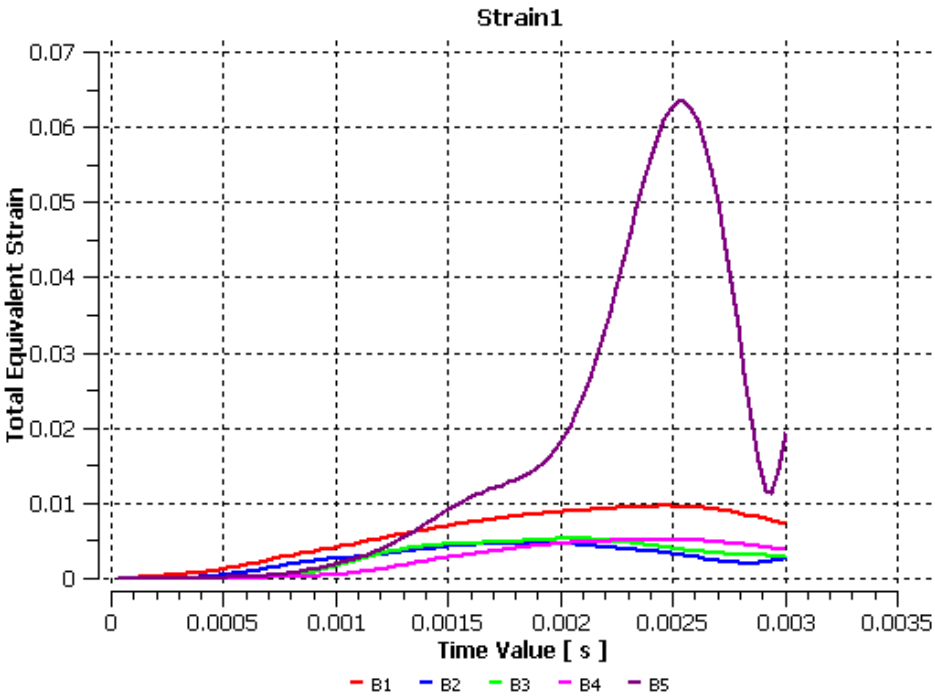

Figure A 10 Total Equivalent Strain of the Brain

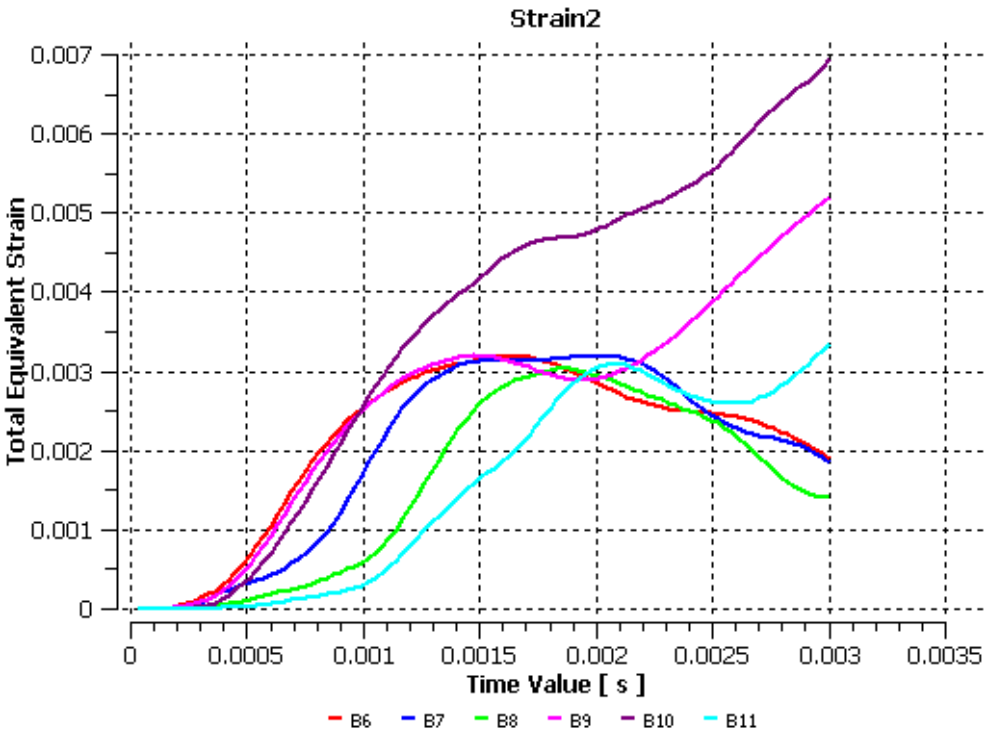

Figure A 11 Total Equivalent Strain of the Brain

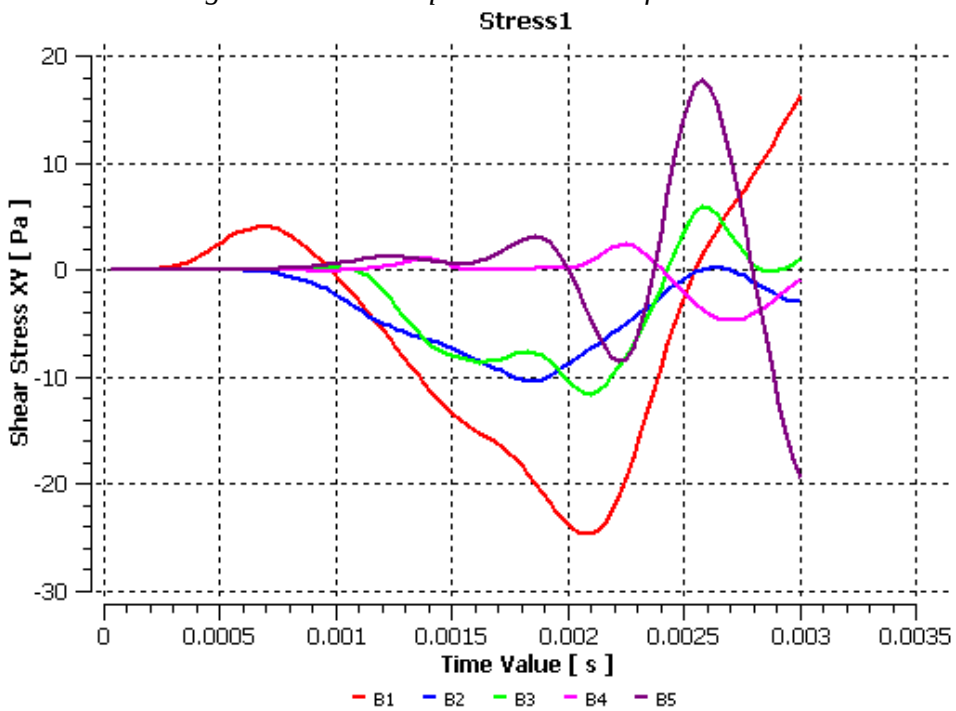

Figure A 12 Shear Stress of the Brain

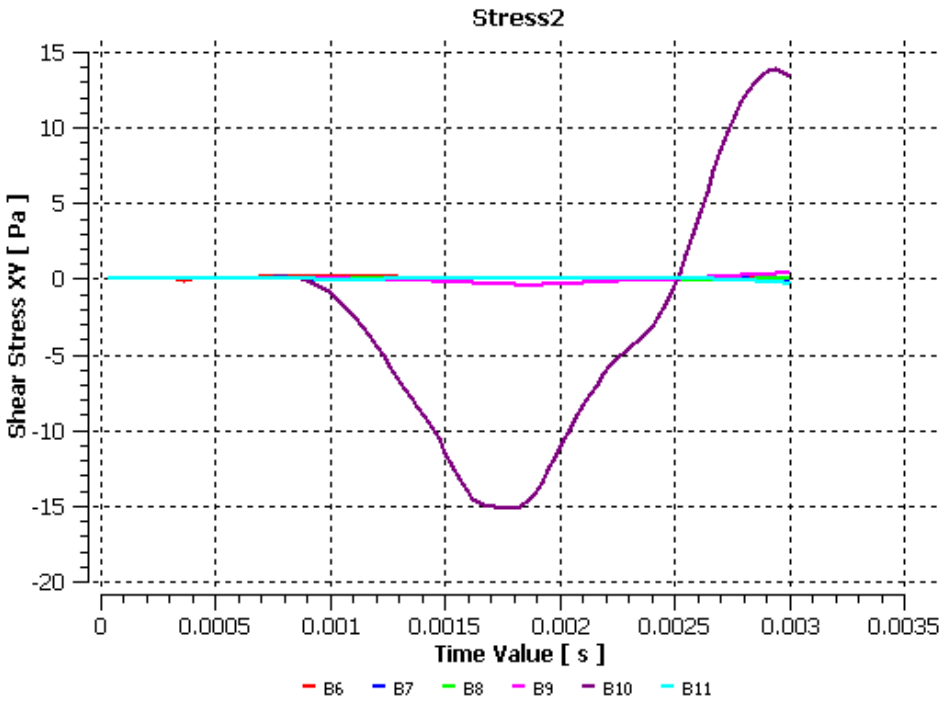

Figure A13 Shear Stress of the Brain

Simulation 2

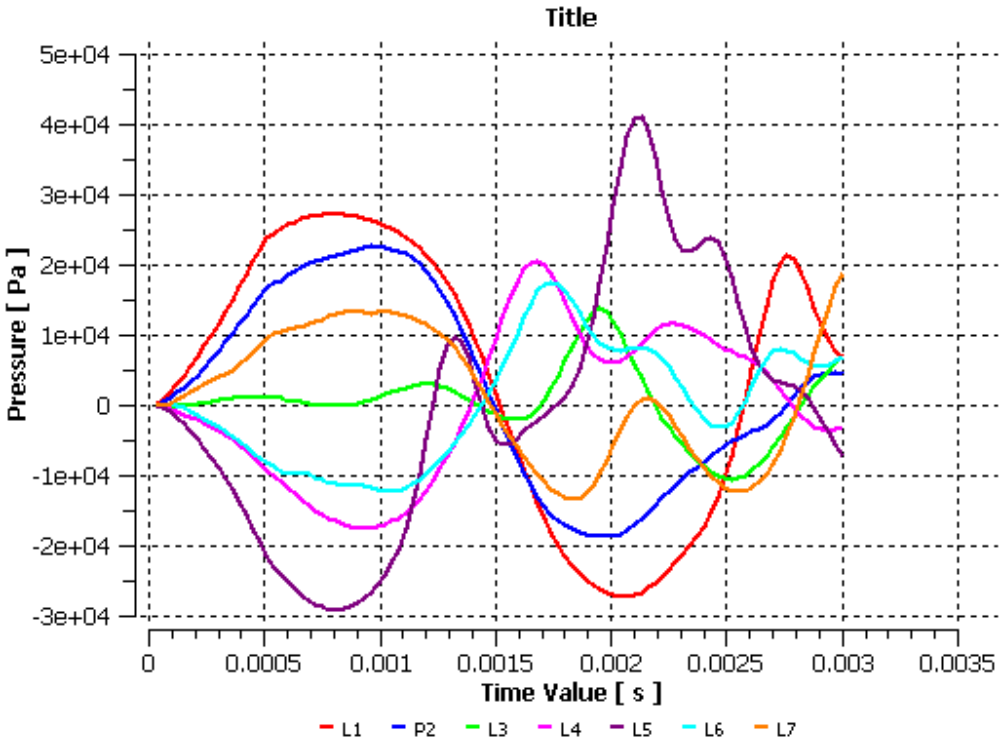

Figure A 14 Pressure inside the CSF

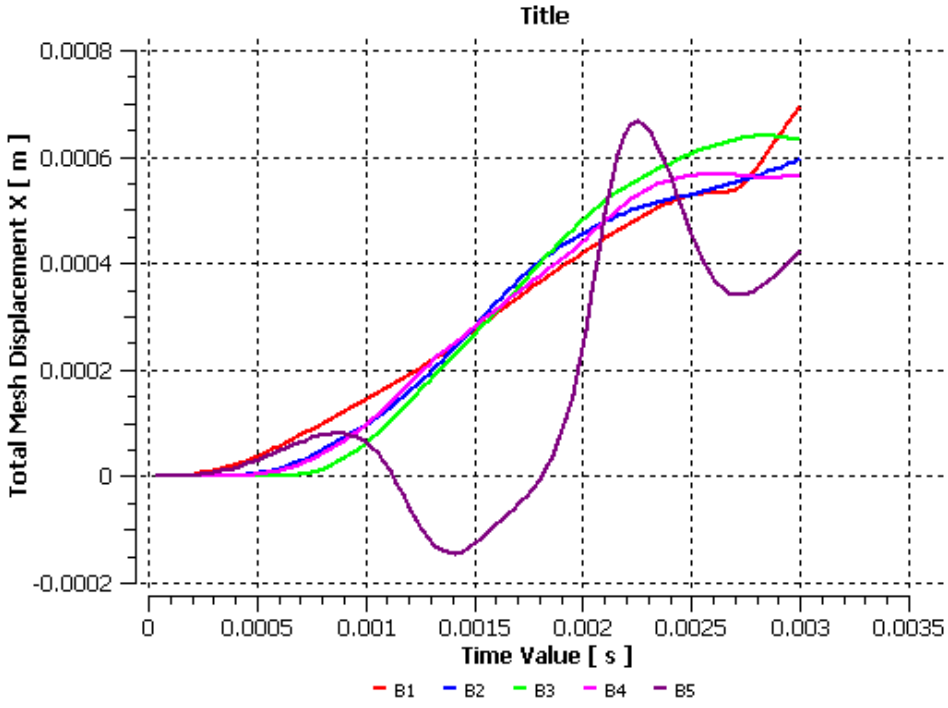

Figure A 15 Total mesh displacement in X direction inside the Brain

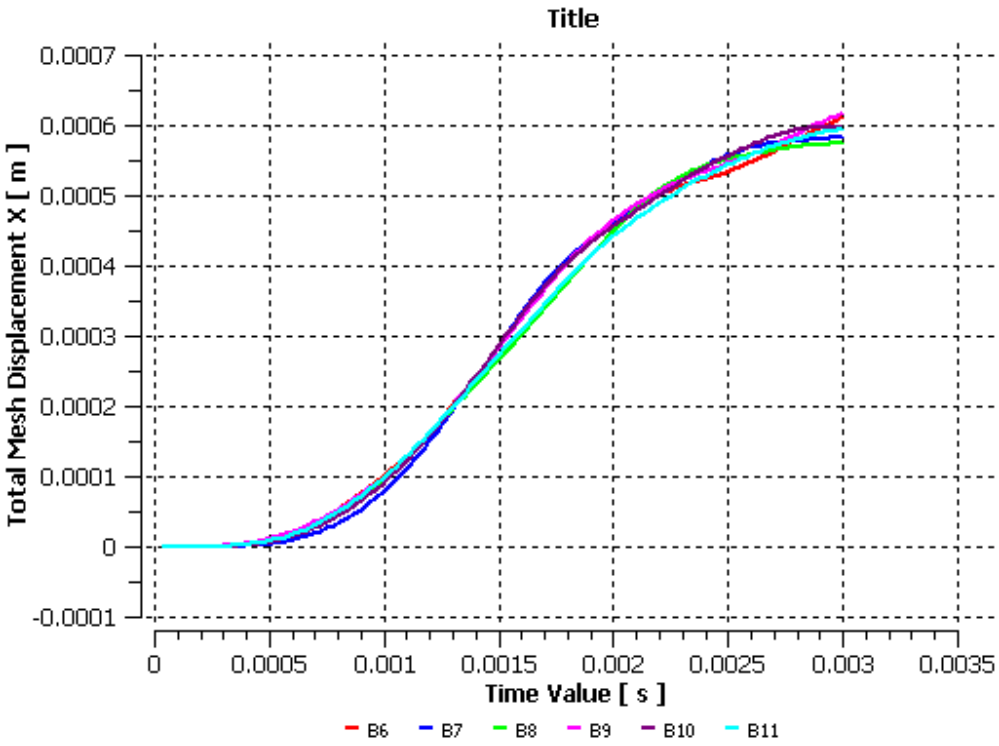

Figure A 16 Total mesh displacement inside the Brain

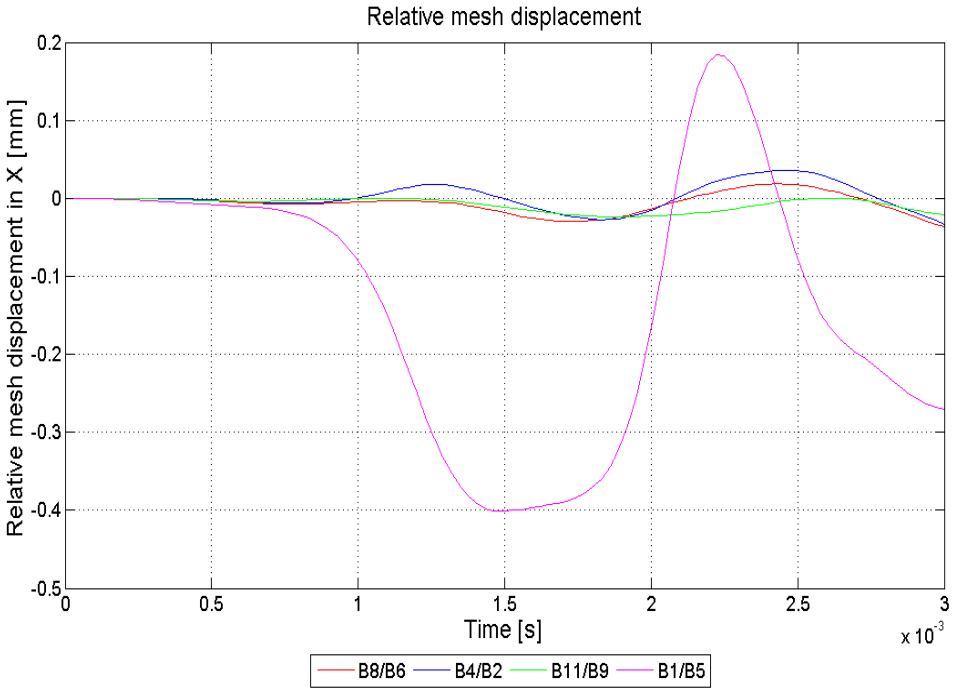

Figure A 17 Relative mesh displacement in X direction of the brain

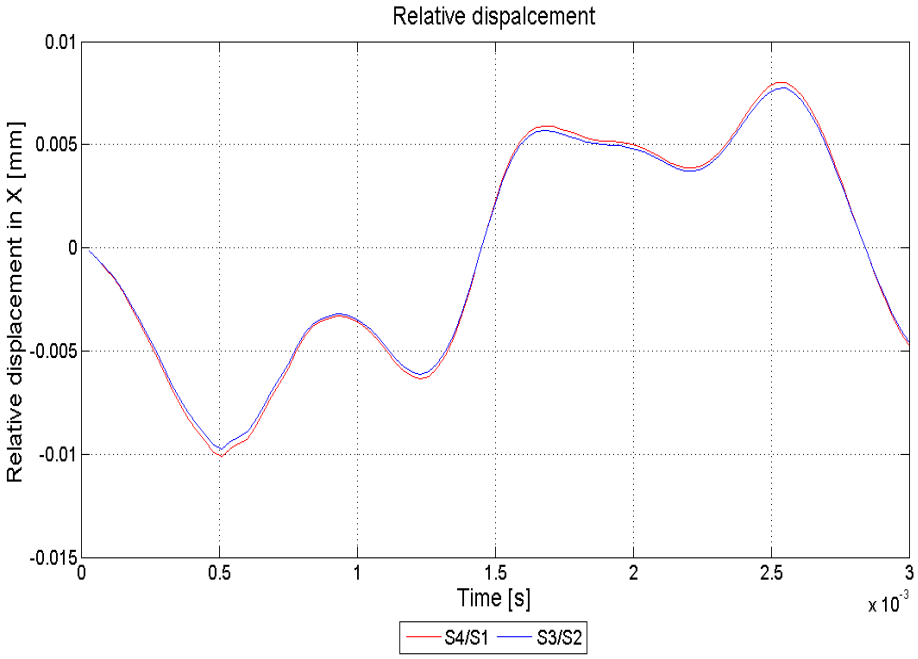

Figure A 18 Relative displacement in X direction of the skull

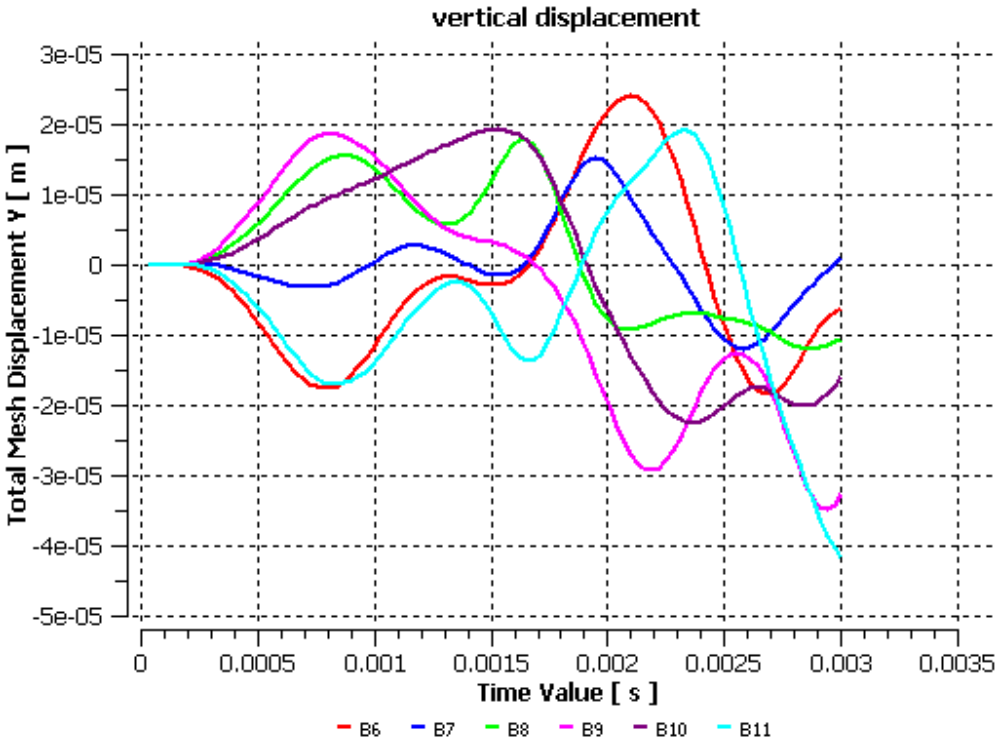

Figure A 19 Total mesh displacement in Y direction of the Brain

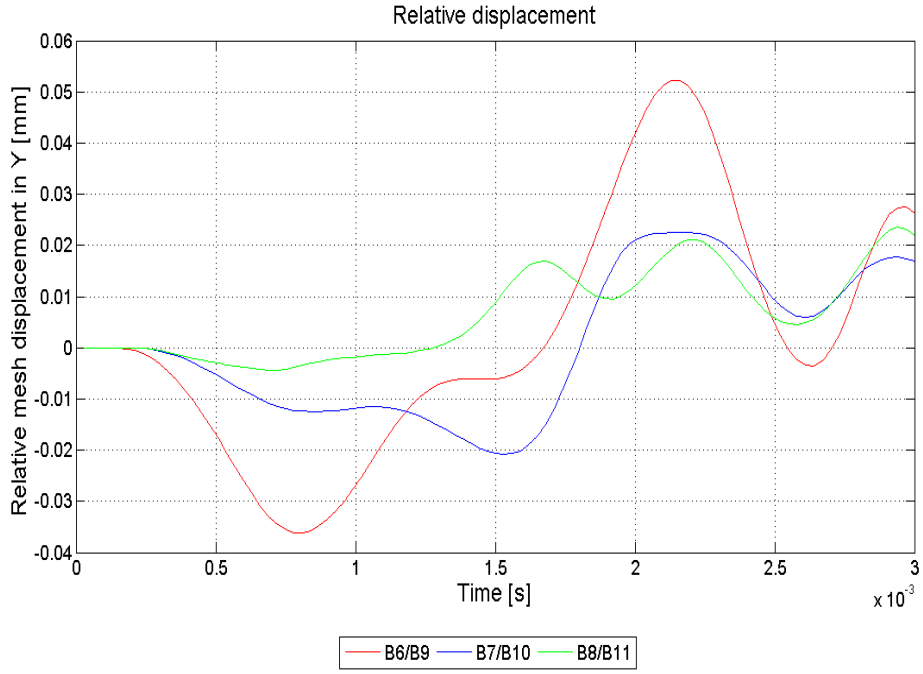

Figure A 20 Relative mesh displacement in Y direction of the Brain

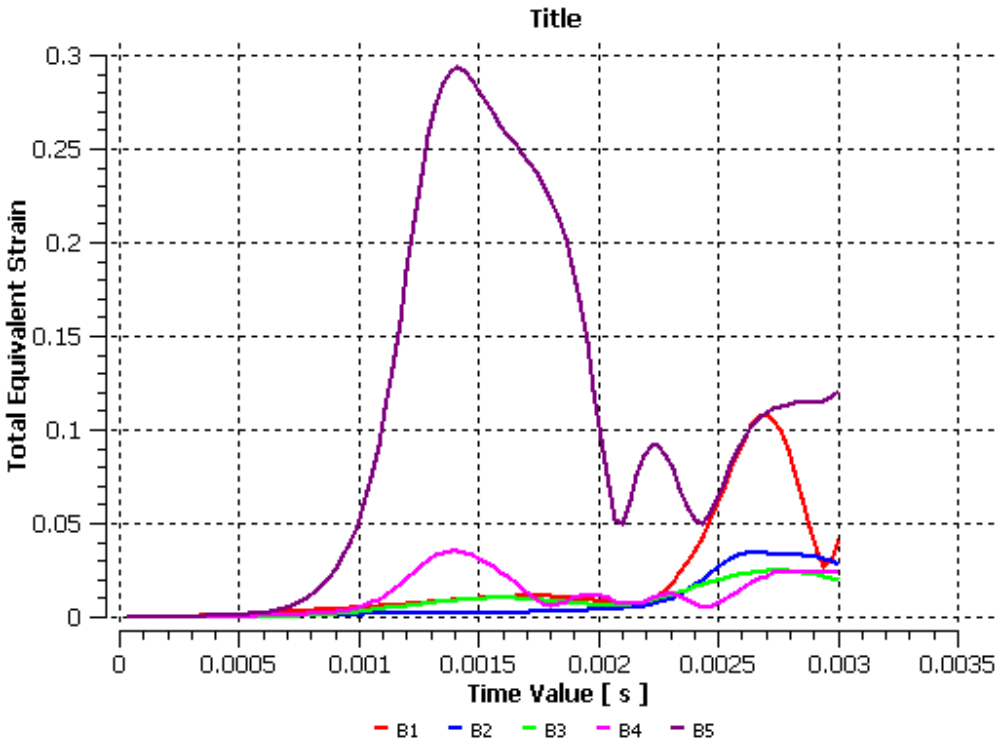

Figure A 21 Total equivalent Strain inside the brain

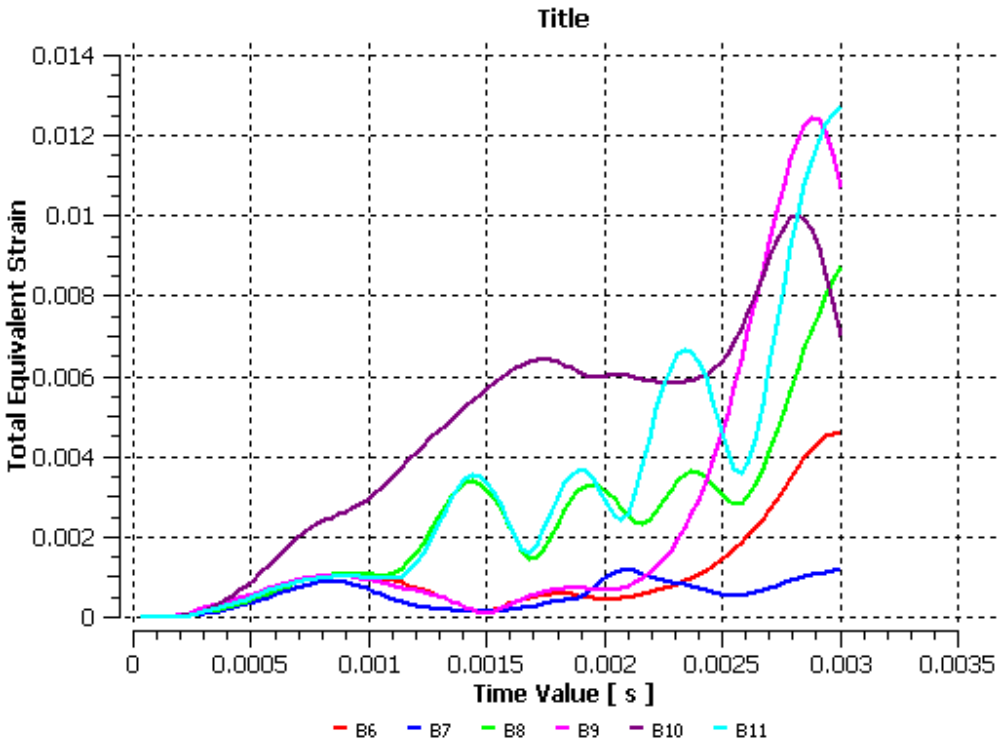

Figure A 22 Total equivalent Strain inside the brain

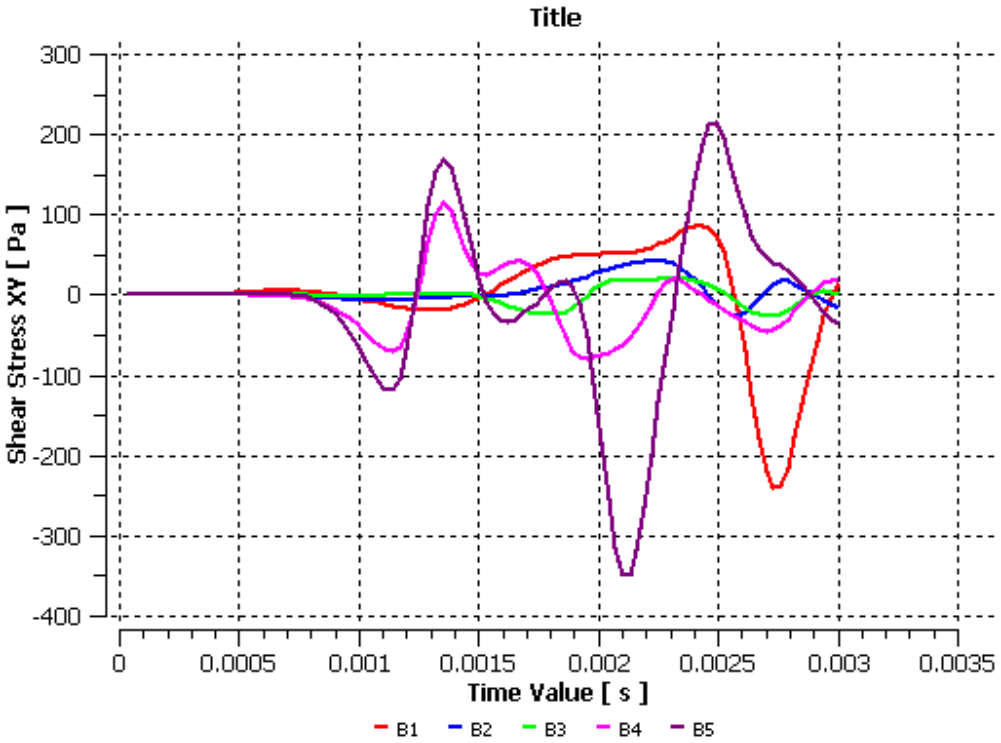

Figure A 23 Shear stress inside the brain

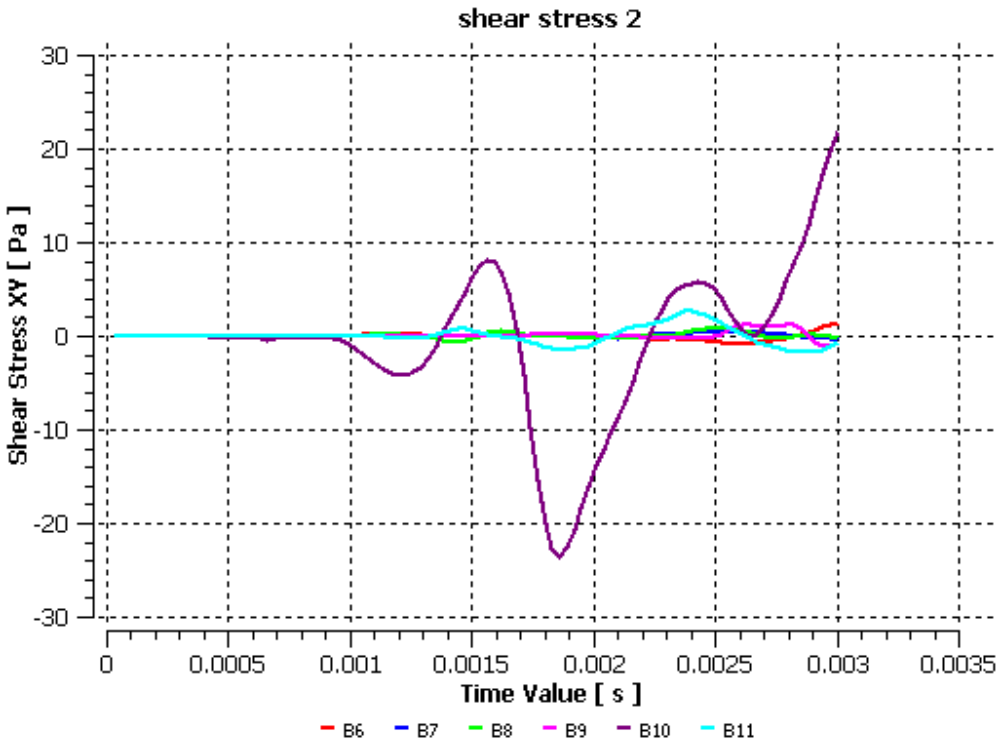

Figure A 24 Shear stress inside the brain